Master of Science Thesis in Electrical Engineering
Department of Electrical Engineering, Linköping University, 2019

Full Cycle Cylinder State Estimation in DI Engines with VVA

Linus Johansson

LINKÖPING UNIVERSITY

Master of Science Thesis in Electrical Engineering

Full Cycle Cylinder State Estimation in DI Engines with VVA

Linus Johansson

LiTH-ISY-EX--19/5221--SE

Supervisor: **Max Johansson**
ISY, Linköping University
Erik Höckerdal
Scania CV AB

Examiner: **Lars Eriksson**
ISY, Linköping University

Division of Automatic Control
Department of Electrical Engineering
Linköping University
SE-581 83 Linköping, Sweden

Sammanfattning

Högre ställda krav på emissioner kräver bättre förståelse för förloppen inom cylindern. Cylindermodellen som tagits fram inom exjobbet bidrar med att kunna använda samma uppsättning ekvationer för förloppen insug, kompression, expansion/förbränning och avgastakt. En cylindermodell med tillstånden temperatur, tryck och massfraktion luft har tagits fram.

Modellen hanterar gasväxling via variabla kompressibla flöden för ventiler där kamfasning, dekompressionsbroms och blowby hanteras. Föbränning modelleras med en enkel Vibefunktion som beskriver värmefrigörelsen samt konsumption av luft.

Modellen är gjord för att vara generell och kunna användas på såväl SI som CI motorer. De kalibreringar som behövs är strömmningsmotståndskoefficient C_D för avgas, insugsventil och blowby samt parametrar för värmeöverföring / frigörelse. Dessutom måste olika motorgeometriparametrar sättas för att kunna räkna ut den momentana cylindervolymen. Modellen har visat god överensstämelse för cylindertryckkurvor med och utan förbränning där ventilerna fasats olika mycket. Det visar att den kan hantera de viktiga fallen som förekommer i förbränningsmotorer. Det går med enkelhet att ersätta delmodeller i modellen t.ex. enkel Vibe mot dubbel Vibe. En utsignal är Φ i cylindern, dessutom räknas skattat indikerat medelmoment för hela motorn fram utifrån tillstånden i en cylinder. Dessa två uträkningar har stämt väl överens med stationära mätningar utförda i motorprovcell. Modellen klarar av fix steglängd för jämn processorlast, steglängderna har varit tillräckligt långa för att modellen rimligen kan användas för realtidsimplementering på motorstyrenhet.

Abstract

Tougher legal demands on pollutions require a better developed understanding of the processes that take place in the cylinder. The thesis contributes with a cylinder model that uses the same set of equations for intake, compression, expansion/combustion and exhaust. The cylinder model describes the states temperature, pressure and the mass fraction of air.

The model is able to simulate the gas exchange with compressible flows over the valves, it handles VVT, CRB and blowby. The combustion is modeled with a single Vibe function that describes the heat release and the consumption of air.

The model is general enough to be able to simulate both SI and CI engines. The calibrations that are needed are the discharge coefficient C_D values for intake and exhaust valves, blowby, and heat release/transfer parameters. Furthermore, the engine geometry parameters have to be provided to be able to calculate the instanteneous cylinder volume. The model has shown good agreement for cylinder pressure curves with and without combustion and can handle phasing of the valve lifts. That shows that the model can handle the important cases in combustion engines. It is easy to replace sub models in the cylinder model e.g. single Vibe with double Vibe. In the model, Φ in the cylinder is calculated and the average instantenous torque for the entire engine is calculated from the states in one cylinder. These two calculations have shown good agreement with the stationary measurments done in an engine test cell. The model is able to use fixed step lengths for even processor loads, the size of the step lengths are resonable for real time implementation on an ECU.

Acknowledgments

I would like to show my gratitude to my family and especially my girlfriend Matilda for always believing in me and for all support during the past years. I would like to thank all friends I have made during my studies in Linköping. Without you I would not have come this far. I would like to thank Scania CV AB for the opportunity of writing this thesis and especially my supervisor at Scania Erik Höckerdal for all the guidance and for always having time for discussion. I would also like to thank all my collegues at NCPP for the coffee breaks and interesting discussions. I would also like to show my gratitude to my examiner Lars Eriksson for introducing me to the exciting world of automotive engineering and finally a big thank you to my supervisor at ISY Max Johansson.

Södertälje, June 2019
Linus Johansson

Contents

Notation

Abbreviations

Abbreviation	Description
AMB	Ambient
BDC	Bottom Dead Center
CA	Crank Angle
CHEPP	Chemical Equilibrium Program Package
CI	Compression Ignited
CN	Cetane Number
CRB	Compression Release Brake
DI	Direct Injected
DS	Downstream
ECU	Engine Control Unit
EGR	Exhaust Gas Recirculation
EVC	Exhaust Valve Closing
EVO	Exhaust Valve Opening
HIL	Hardware in the Loop
HLA	Hydraulic Lash Adjusters
HT	Heat Transfer
HR	Heat Release
ICE	Internal Combustion Engine
IVC	Intake Valve Closing
IVO	Intake Valve Opening
MFB	Mass Fraction Burned
MVEM	Mean Value Engine Models
SI	Spark Ignited
SOC	Start Of Combustion
SOI	Start Of Injection
TDC	Top Dead Center
US	Upstream
VVA	Variable Valve Actuation
VVT	Variable Valve Timing

Constants

Constant	Description
A_R	Reference Area [m^2]
$(A/F)_s$	Stoichiometric Air/Fuel Ratio [-]
$(F/A)_s$	Stoichiometric Fuel/Air Ratio [-]
n_{cyl}	Number Of Cylinders [-]
M	Molar Mass [g/mole]
p_{amb}	Ambient Pressure [Pa]
T_{amb}	Ambient Temperature [K]
Q_{LHV}	Lower Heating Value [MJ/kg]
$\tilde{R} = 8.3143$	Gas Constant [J/(mol K)]

Variables

Variable	Description
A_E	Effective Area [m^2]
C_D	Discharge Coefficient [-]
$\tilde{c}_v$	Specfic Heat At Constant Volume [J / (mole K)]
c_v	Mass Specfic Heat At Constant Volume [J / (kg K)]
$\tilde{c}_p$	Specfic Heat At Constant Pressure [J / (mole K)]
c_p	Mass Specfic Heat At Constant Pressure [J / (kg K)]
D_v	Valve Head Diameter [mm]
E_A	Activation Energy [J/mole]
L_v	Valve Lift [mm]
M_e	Engine Torque [Nm]
m_f	Mass Fuel Injected [kg]
n	Number of Moles [mole]
N_e	Engine Speed [rpm]
p_m	Motored Pressure [Pa]
p	Pressure [Pa]
Q	Heat [W]
T	Temperature [K]
V	Volume [m^3]
$\bar{S}_p$	Mean Piston Speed [m/s]
x_b	MFB [-]
x	Mass fraction [-]
$\tilde{x}$	Mole fraction [-]
η_{co}	Combustion Efficiency [-]
$\gamma = \frac{c_p}{c_v}$	Specific Heat Ratio [-]
κ	Polytropic Exponent [-]
τ_{id}	Ignition Delay [CA]
ω_e	Engine Speed [rad/s]
λ	Air Fuel Ratio [-]
Φ	Fuel Air Ratio [-]

1 Introduction

In the coming years the legislation will be tougher on pollution from vehicles. In Åkerman (2019) it is described that the EU parliament have decided that the CO_2 emissions for new trucks will have to decrease by 30% from the levels emitted in 2019 until 2030. To achieve this a further understanding of the physical phenomena that take place inside the cylinder is vital. Therefore a model that can estimate the state of the cylinder is needed. The understanding of the process in the cylinder gives tools to improve the fuel economy. That is of great interest since the fuel is a major part of the cost of maintaining a truck. The contribution of this thesis is to use the same model structure for all the different phases in the full four stroke cycle. Previous work has mostly been either on the open cycle where there is gas exchange or on the closed cycle when the valves are closed.

1.1 Objectives

The objective of this thesis is to model the cylinder pressure trace and other thermodynamic states over the full cycle in a CI engine. The goal is that the model will handle special cases like cam phasing, Variable Valve Timining (VVT) and how it affects the gas exchange. The model will also have a combustion and heat transfer model and include contributions from blowby. The model will be as generic as possible so that the structure with small modifications can be used when simulating cylinder states in SI engines.

1.2 Delimitations

Items that are outside the scope of this thesis are:

- Multi-zone combustion models
- EGR
- Fuel spray models
- Crevice effects
- Thermal stress and solid mechanics that affects cylinder volume calculations.
- Warm up process of the engine.
- Formation of emissions.
- Data collection on different engines.
- Implementation of a control system.

1.3 Related Work

Previous work on cylinder pressure have most often used the cylinder pressure for studying the heat release. That has been done in several works for example Gatowski et al. (1984), Klein (2007) and Egnell (2000). In those works the heat transfer most often uses the empirical observation made by Woschni (1967). Modeling the cylinder pressure have been made in Eriksson and Andersson (2002). There, an analytical cylinder pressure model was developed for an SI-engine. That model did not rely on solving differential equations in each step. However that model does not take heat transfer directly into account or the effect that the gas properties changes when there is internal EGR (residual gases) and change in temperature. The model needs to be fitted to many different cases. Templin (2002) used a crank angle based cylinder pressure model for modeling compression release brake (CRB). In the article it was argued that CRB takes place during one cycle and therefore needs a crank based pressure model. The intention of this thesis is to also model CRB in the same framework.

The combustion is most often modelled by Vibe functions presented in Vibe and Meißner (1970). The idea in this thesis is to use a single Vibe function to make a simple combustion model. The Vibe function is parameterized by studying the heat release. The heat release can be obtained from the cylinder pressure data by methods described by Krieger and Borman (1966), Rassweiler and Withrow (1938) and Sellnau et al. (2000). Klein (2007) mentions that Matekunas pressure ratio concept has been shown to be able to predict MFB50 accurately.

1.4 Thesis Outline

In Chapter 1 the motivation of the thesis is presented and the work is put in relation to previous work. Chapter 2 will describe the necessary theory to model the cylinder pressure. Chapter 3 will provide a description on how the model

is implemented and the different algorithms used to estimate parameters. In Chapter 4 the data collection and the limitations of some sensors are discussed. In Chapter 5 the results will be presented and discussed and finally in Chapter 6 future work will be discussed.

2
Theory

In this chapter the relevant theory needed when modeling the thermodynamic cylinder states for a four stroke CI engine is presented. Much of the theory presented in this chapter is also applicable for SI engines.

2.1 The Four Stroke Cycle in a CI-Engine

The four strokes in a CI-engine is explained below and is visualised in Figure 2.1.

1. **Intake** This is when the intake valve is opened and the cylinder is filled with air. During the intake the cylinder pressure is close to the pressure in the intake manifold. The piston moves from TDC to BDC.

2. **Compression** The valves are closed and the air is compressed to a higher pressure and temperature when the piston moves towards TDC. Fuel is injected towards the end of the compression stroke. Combustion starts when the fuel in the charge have diffused sufficiently with the air. The combustion continues through the power stroke.

3. **Power stroke** Work is performed by the fluid during the power stroke when the volume increases. When the exhaust valve is opened the blowdown starts. The cylinder pressure decreases as the fluid is blown out to the exhaust system.

4. **Exhaust** The fluid is pushed out to the exhaust when the piston moves toward TDC again. The cylinder pressure is close to the pressure in the exhaust manifold. After this process the cycle is complete and it starts over with the intake.

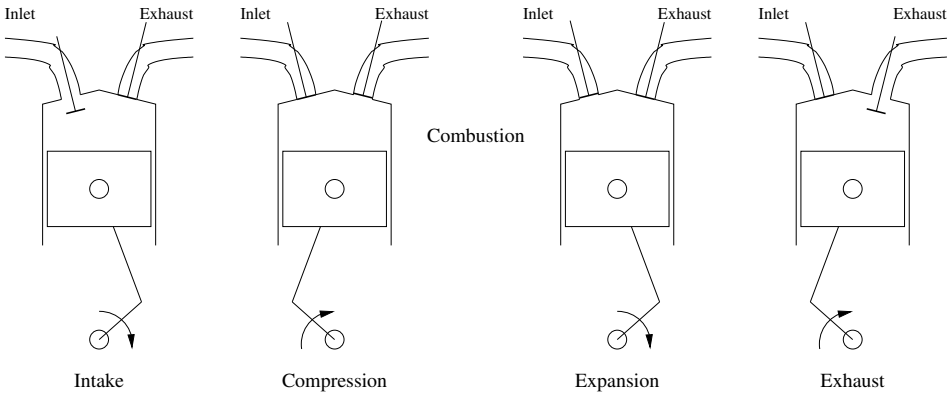

Figure 2.1: *The four strokes. Reprinted with permission from Eriksson and Nielsen (2014).*

2.2 Engine Geometry

The cylinder's instantaneous volume is calculated from crank angle and engine geometry data, shown in the equations below. The notation in the equation follows the notation in Figure 2.2 and Table 2.1.

Table 2.1: *Names and notation from the engine geometry from Figure 2.2.*

Name	Notation
Cylinder Bore	B
Crank angle	θ
Connecting rod length	l
Crank radius	a
Piston stroke	L = 2a
Clearance volume	V_c
Displaced volume	V_d
Top Dead Center	TDC
Bottom Dead Center	BDC

The equations that follows for calculating volume or surface area uses the same notation as in Figure 2.2.

The displaced volume for one cylinder is:

$$V_d = \frac{\pi B^2 L}{4}. \tag{2.1}$$

The total displacement of the entire engine with n_{cyl} cylinders is:

$$V_D = n_{cyl} V_d. \tag{2.2}$$

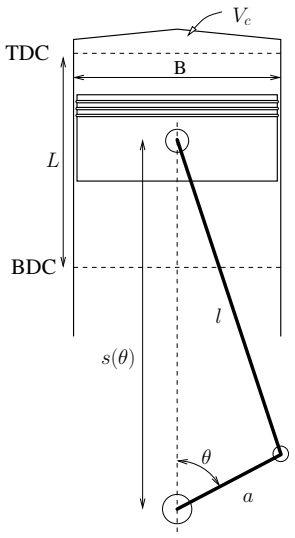

Figure 2.2: *The engine geometry. Reprinted with permission from Eriksson and Nielsen (2014).*

The compression ratio can be calculated with:

$$r_c = \frac{\text{maximum cylinder volume}}{\text{minimum cylinder volume}} = \frac{V_d + V_c}{V_c} \tag{2.3}$$

The instanteneous volume of one cylinder as an expression of the crank angle θ:

$$V(\theta) = V_d \left(\frac{1}{r_c - 1} + \frac{1}{2} \left(\frac{l}{a} + 1 - \cos(\theta) - \sqrt{\left(\frac{l}{a}\right)^2 - \sin^2(\theta)} \right) \right) \tag{2.4}$$

The derivative of equation (2.4) is:

$$\frac{dV(\theta)}{d\theta} = \frac{1}{2} V_d \sin(\theta) \left(1 + \frac{\cos(\theta)}{\sqrt{\left(\frac{l}{a}\right)^2 - \sin^2(\theta)}} \right) \tag{2.5}$$

Equation (2.5) can be calculated in the time domain with usage of the chain rule

$$\frac{dV(\theta)}{dt} = \frac{dV(\theta)}{d\theta} \underbrace{\frac{d\theta}{dt}}_{\omega_e} = \frac{dV(\theta)}{d\theta} \omega_e. \tag{2.6}$$

The area of the combustion chamber, piston crown and cylinder head depending on θ:

$$A(\theta) = (l + a - s(\theta))\pi B + \frac{2\pi B^2}{4} \tag{2.7}$$

$$s(\theta) = a\cos(\theta) + \sqrt{l^2 - a^2\sin^2(\theta)} \tag{2.8}$$

The area is of interest when calculating the heat transfer. There is however simplifications on calculating the instantaneous volume based on engine geometry. During the engine operation the components around the combustion chamber are exposed to thermal forces and pressure forces. These forces will deform the components which will make the volume deviate from the ideal. In Anagrius West et al. (2018) it was concluded that the instantaneous volume can deviate as much as 6% from the geometrical at TDC. That study was conducted on an inline six cylinder Scania engine.

2.3 Ideal Gas

An equation of states is an equation that relates pressure p, temperature T and volume V as

$$f(p, T, V) = 0 \tag{2.9}$$

The most common equation of states is the ideal gas law

$$pV = n\tilde{R}T = m\frac{\tilde{R}}{M}T = mRT \tag{2.10}$$

The ideal gas law can either be expressed in moles or with mass. R in the equation depends on what type of gas it is while $\tilde{R}$ is a constant.

It has been shown experimentally that real gases obey the ideal gas law at low densities. Many gases behave as ideal gases in intervals used in engineering applications and the ideal gas assumption can be made with small errors. There are other equations of state for example Van der Waals equation which is more accurate than the ideal gas law for real gases. At small densities Van der Waals equation reduces to the ideal gas law. However these equations of states cannot handle transition from gas to liquid (Cengel et al., 2017).

Heywood (2019) concludes that the gas species that makes up the working fluid in ICE usally can be treated as ideal gases.

2.4 Thermodynamic States

The first law of thermodynamics describes the rate of change for the internal energy see eqution (2.11). $\dot{H}$ describes the enthalpy flow, $\dot{Q}$ describes the heat relase and heat transfer. $\dot{W}$ describes the mechanical power from $p\frac{dV}{dt}$.

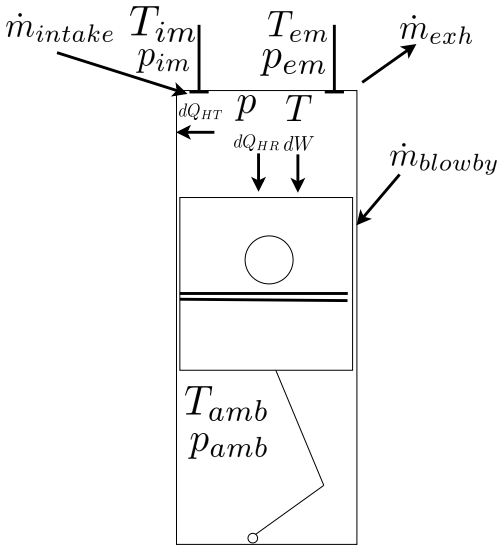

Figure 2.3: *The flows in and out of the cylinder.*

In Figure 2.3 the flows in to the cylinder are shown. The flows are taken as postitive if they flow as in the Figure while they are negative if they flow in the opposite direction.

The first law of thermodynamics for the system in Figure 2.3 is

$$\frac{dU}{dt} = \sum_i \dot{H}_i - \dot{Q} - \dot{W} \tag{2.11}$$

In equation (2.11) i denotes the different flows to and from the cylinder. The flows are defined as in Figure 2.3.

The enthalpy flow is described by the following relation

$$\dot{H} = \dot{m} c_p T \tag{2.12}$$

In the single zone model the enthalpy flow will be replaced with the specific enthalpy and massflows.

$$\dot{H} = h\dot{m} \tag{2.13}$$

Considering thermodynamic relations the internal energy can be expressed as the following:

$$U = m c_v dT \tag{2.14}$$

By differentiating the internal energy an expression for the temperature diffrential can be obtained see equation (2.15).

$$\frac{dU}{dt} = \frac{d(mu)}{dt} = \sum_i u(T)\frac{dm_i}{dt} + m\frac{du}{dt}$$
$$\overbrace{=}^{\text{Eq: (2.14)}} \sum_i u(T)\frac{dm_i}{dt} + mc_v\frac{dT}{dt} \tag{2.15}$$

By inserting equation (2.15) into (2.11) equation (2.16) is obtained.

$$mc_v\frac{dT}{dt} = \sum_i (h_i' - u)\frac{dm_i}{dt} - \frac{dQ}{dt} - \frac{dW}{dt}$$
$$\frac{dT}{dt} = \frac{RT}{pVc_v}\left(\sum_i (h_i' - u)\frac{dm_i}{dt} - \frac{dQ}{dt} - p\frac{dV}{dt}\right) \tag{2.16}$$

In the last step the ideal gas law have been used to remove m from the equation. u is the internal energy of the cylinder, h' is the mass specific enthalpy and it is evaluated from where the flow origins (Heywood, 2019).

To get an expression for the pressure the ideal gas law in equation (2.10) is diffrentiated.

$$V\frac{dp}{dt} + p\frac{dV}{dt} = RT\sum_i \frac{dm_i}{dt} + mR\frac{dT}{dt}$$
$$\frac{dp}{dt} = \frac{RT}{V}\sum_i \frac{dm_i}{dt} - \frac{p}{V}\frac{dV}{dt} + \frac{p}{T}\frac{dT}{dt} \tag{2.17}$$

Thereby temperature and pressure is selected as the two states according to equation (2.18).

$$\begin{bmatrix} \frac{dT}{dt} \\ \frac{dp}{dt} \end{bmatrix} = \begin{bmatrix} \frac{RT}{pVc_v}\left(\sum_i (h_i' - u)\frac{dm_i}{dt} - \frac{dQ}{dt} - p\frac{dV}{dt}\right) \\ \frac{RT}{V}\sum_i \frac{dm_i}{dt} - \frac{p}{V}\frac{dV}{dt} + \frac{p}{T}\frac{dT}{dt} \end{bmatrix} \tag{2.18}$$

In the derivation of the thermodynamic states crevice effects have been neglected since the engine is Direct Injected (DI). In DI engines the fuel is injected into a cavity in the piston and it is thereby kept from entering crevices (Johansson, 2017). Crevices are regions where fuel can enter and avoid combustion. In port injected engines crevice effects has to be considered since the air and fuel is premixed and the flame does not reach the fuel in the crevices (Heywood, 2019). Other assumptions made in this derivation is that the temperature is homogenous in the entire cylinder.

The ideal gas can be used to calculate the mass that is trapped in the cylinder as

$$m = \frac{pV}{RT} \tag{2.19}$$

2.5 Gas Properties

The gas composition in the cylinder is considered to be a pure substance. A pure substance means that the gas composition is homogenous. A commonly used assumption for ICE is that the working fluid is air. It is called the air-standard assumtion (Cengel et al., 2017). The assumption is as follows:

1. The working fluid is air, which is circulated in a closed loop and always behaves as an ideal gas.
2. All processes that make up the cycle are internally reversible.
3. The combustion process is replaced by an external heat addition.
4. The exhaust process is replaced by a heat rejection process that restores the working fluid to its initial state.

2.5.1 Air

Air is a mixture of many gases and the most vital element for combustion is oxygen. Oxygen is essential for engines since it oxidizes the fuel and it is the oxidation process that releases energy. The other gases are inert gases and have minor effects on the combustion but they take up heat and space in the combustion chamber. A commonly used model for air is discussed in Eriksson and Nielsen (2014) and it is to assume that air only consist of oxygen and nitrogen. Neglecting the other molecules present in air will lead to a small error, however this error can be reduced if the other gases are lumped into nitrogen. The consideration that all molecules are nitrogen except oxygen gives that there are 3.773 nitrogen molecules for each oxygen molecule. This leads to the following model for air:

$$\text{Air} = O_2 + 3.773N_2 \tag{2.20}$$

2.5.2 Gas Relations

In thermodynamical systems the specific heat ratio is often used, it is defined as

$$\gamma = \frac{c_p}{c_v}. \tag{2.21}$$

Assuming that a gas is ideal, gives the following relation between mass specific heats and the mass specific gas constant $R = c_p - c_v$.

The mole fraction $\tilde{x}$ for specie i is defined as

$$\tilde{x} = \frac{n_i}{n} \tag{2.22}$$

n is the total amount of moles of all species in the entire gas and n_i is the amount of moles of specie i.

The mass fraction x for specie i is defined as

$$x_i = \frac{m_i}{m_{tot}} \tag{2.23}$$

m_i is the mass of specie i and m_{tot} is the total mass.

For a gas consisting of several molecules where the mole/mass fraction $\tilde{x}_i/x_i$ is known the $\tilde{c}_p/c_p$ value for the gas can be obtained by the following:

$$\tilde{c}_p = \sum_i \tilde{x}_i \tilde{c}_{p,i} \tag{2.24a}$$

$$c_p = \sum_i x_i c_{p,i} \tag{2.24b}$$

The relation from mole fraction to mass fraction is the following

$$x_i = \frac{m_i}{m} = \frac{\tilde{x}_i M_i}{\sum_j \tilde{x}_j M_j} \tag{2.25}$$

The relation from mass fraction to mole fraction is the following

$$\tilde{x}_i = \frac{n_i}{n} = \frac{x_i/M_i}{\sum\limits_j x_j/M_j} \tag{2.26}$$

The molecular weight of a gas containing different chemical species is needed to be able to get the thermodynamic properties on a mass basis. In the equation below M_i is the molar mass of substance i, n_i is how many moles there are of substance i and finally n denotes the total amount of moles of the different mixtures in the gas.

$$M = \frac{1}{n} \sum_i n_i M_i = \sum_i \tilde{x}_i M_i \tag{2.27}$$

The scaling from molar basis to mass basis is the following

$$n = \frac{m}{M} \tag{2.28}$$

$$m = nM \tag{2.29}$$

Thereby all thermodynamic properties can be obtained in either molar basis or in mass basis and then be converted to the other.

$$R = \frac{\tilde{R}}{M} \tag{2.30}$$

Given the ideal gas assumption c_p and c_v can be expressed in R and γ according to

$$c_v = \frac{R}{\gamma - 1} \tag{2.31}$$

$$c_p = \frac{R\gamma}{\gamma - 1}. \tag{2.32}$$

The air/fuel equivalence ratio λ has the following definition

$$\lambda = \frac{m_{air}}{m_{fuel}(A/F)_s} \tag{2.33}$$

$(A/F)_s$ is the stochiometric air/fuel ratio. It tells the relation between the amount of air and fuel to have stochiometric reaction which between hydrocarbons and air only produces H_2O and CO_2. When there is excess air in the combustion, i.e. $\lambda > 1$, the mixture is said to be lean. If $\lambda < 1$ and there is excess fuel the mixture is said to be rich.

It is also common to use Φ which is λ^{-1}.

$$\Phi = \lambda^{-1} = \frac{m_{fuel}}{m_{air}(F/A)_s} \tag{2.34}$$

The benefit of using Φ instead of λ is that Φ can handle when $m_{fuel} = 0$. In the Φ model a saturation is that Φ has its lowest value as 0.01 which means that $\lambda = 100$ for cases with absense of combustion.

2.5.3 NASA Polynomials

The specific heat ratio will depend on temperature and a common way to model that is to use NASA polynomials. NASA polynomials is a database where polynomials have been fitted for different chemical species. The equations for the NASA polynomials look like equation (2.35) where the coefficients varies depending on which chemical specie it is (J. McBride et al., 2002).

$$\frac{\tilde{c}_p(T)}{\tilde{R}} = a_1 + a_2 T + a_3 T^2 + a_4 T^3 + a_5 T^4 \tag{2.35}$$

The NASA polynomials are specified for the common chemical species in temperature ranges 300-1000 K and 1000-5000 K. The coefficients in the NASA polynomials are different in those temperature ranges and are different for various chemical species. To obtain the $\tilde{c}_p$ for the whole gas equation (2.24a) is used.

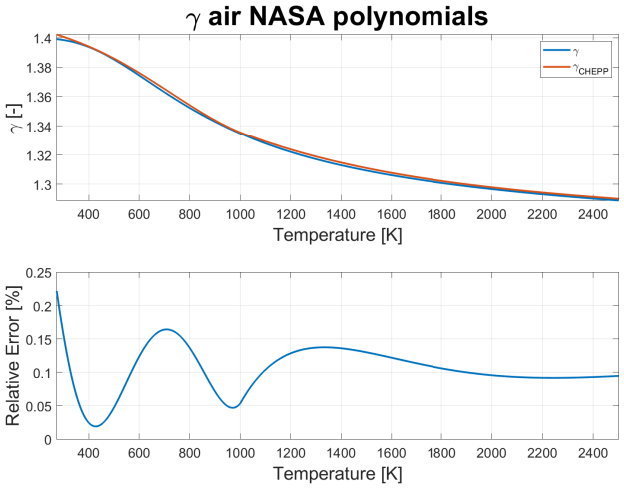

Figure 2.4: *γ for air dependent on temperature.*

There is however other thermochemical programs that can be used to model how the gas properties varies with temperature and what chemical elements are present in the gas. One example of such a program is CHEPP. It is a chemical equilibrium package designed for Matlab (Eriksson, 2005). It can calculate thermochemical properties for molecules and for combustion products. CHEPP will in this work be used to benchmark the NASA polynomials and see that the implementation is correctly made. In Figure 2.4 a comparison between CHEPP and NASA polynomials for air is shown. The NASA polynomials have used the simplified model of air according to equation (2.20).

2.5.4 Gatowski's Model

A commonly used model for γ is based on equation (2.36). That model was orignally presented in Gatowski et al. (1984). It has been concluded in Klein and Eriksson (2004) that equation (2.36) is difficult to get precise.

$$\gamma(T) = \gamma_{300} + b(T - 300) \tag{2.36}$$

In Eriksson and Nielsen (2014) it is stated that appropriate values for the constants in equation (2.36) is $\gamma_{300} \approx 1.35$ and that $b \approx 7 \cdot 10^{-5}$.

To be able to parameterize equation (2.36) CHEPP could be used (Eriksson, 2005).

2.6 Gas Exchange

The gas exchange is the breathing of the engine. It is controlled by the camshaft with the camlobes that pushes down the rocker arms which in turn push the

valves. The engine studied in this thesis can change when the camlobes will push down then rocker arms and the valves. It can also add a valve lift for compression release brake (CRB).

2.6.1 Compressible Flow

The flow through poppet valves is often modeled as a compressible flow. This is needed since the gas velocity is high. Components that has small cross section area and large pressure difference are well described by isentropic compressible flow (Eriksson and Nielsen, 2014). For a detailed derivation of compressible flow see (Heywood, 2019, appendix C).

The flow is related to real gas flow effects by experimentally determined discharge coefficients C_D. C_D for the intake and exhaust valves have been measured in an airflow bench. The definition of C_D is the following:

$$C_D = \frac{\text{actual mass flow}}{\text{ideal mass flow}} \tag{2.37}$$

The C_D values and the value of the reference area A_R are linked together, their product is the effective area A_E.

$$A_E = C_D A_R \tag{2.38}$$

The isentropic compressible flow is described by equation (2.39).

$$\dot{m} = \frac{p_{us}}{\sqrt{RT_{us}}} A_E \Psi_{li}\left(\frac{p_{ds}}{p_{us}}\right) \tag{2.39}$$

The index us abbreviation for upstream and means from were the flow origins and ds is an abbreviation for downstream and means where the flow ends. Figure 2.5 shows that γ has negligible impact on the flow function and thereby it is common to use the assumption that γ is a constant.

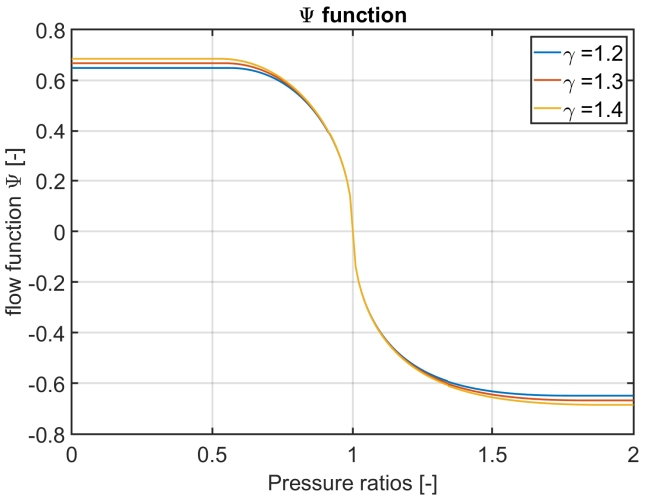

Figure 2.5: *The Ψ function for different γ values.*

Equation (2.40) determines if the flow is choked or not. By choked flow it is meant that the pressure reaches the critical sonic velocity.

$$\Pi\left(\frac{p_{ds}}{p_{us}}\right) = \max\left(\frac{p_{ds}}{p_{us}}, \left(\frac{2}{\gamma+1}\right)^{\frac{\gamma}{\gamma-1}}\right) \tag{2.40}$$

$$\Psi_0(\Pi) = \sqrt{\frac{2\gamma}{\gamma-1}\left(\Pi^{\frac{2}{\gamma}} - \Pi^{\frac{\gamma+1}{\gamma}}\right)} \tag{2.41}$$

Note when the pressure ratio between $\frac{p_{ds}}{p_{us}}$ is close to 1 the model does not fullfill the Lipschitz condition. To be able to fullfill the Lipschitz condition a linear region can be added.

$$\Psi_{li}(\Pi) = \begin{cases} \Psi_0(\Pi) & \text{if } \Pi \leq \Pi_{li} \\ \Psi_0(\Pi_{li})\frac{1-\Pi}{1-\Pi_{li}} & \text{Otherwise} \end{cases} \tag{2.42}$$

The size of the linear region is difficult to determine beforehand. However in Ellman and Piché (1999) a method of determining the size of the linear region is presented. An indication to either add a linear region or to increase it is if there are oscillations present in the simulated mass flow of a component that operates at steady state (Eriksson and Nielsen, 2014). Equation (2.42) can be used to linearize the compressible flow equation. The boundary value when the linear model is used or not is the tuning constant that needs to be investigated.

2.6.2 VVA

The valve event can be altered in any combination of the following (Dresner and Barkan, 1989).

1. Change the advance of valve event, while maintaining the same duration and lift profile.
2. Change valve event duration, while leaving the phase constant.
3. Modify lift characteristic, while leaving phase and duration constant.
4. Retain fixed valve timing and eliminate valve lift completely on selected engine cylinders to vary the effective engine displacement.

The prototype engine used in this thesis can change the phase of the valve event but cannot alter duration. The engine can alter the lift profile by turning on/off the CRB lift profile. There are several benefits in using VVT. It extends the useful engine speed range. VVT can reduce emissions by the improvement in efficiency, because it will require less fuel. For some engines VVT can reduce emissions by controlling the internal EGR. Increasing the internal EGR reduces the combustion temperature and thereby the amount of produced NO_x.

2.6.3 CRB

Simply explained CRB turns the CI-engine into an air compressor. Rather than to store the energy of the pressurised air created when the piston is coming up in the compression stroke, the CRB hydraulically opens the exhaust valve near the end of the upward piston stroke. The stored energy in the cylinder is thus released to the exhaust manifold so when the piston enters the power stroke no pressure remains in the cylinder to act on the piston. The release of the compressed gas dissipates energy and the down movement in the expansion stroke is performed under low pressure which leads to braking torque on the crankshaft (Cummins, 1985). **Note** that CRB is often called Jacobs brake or Jake brake.

2.6.4 Blowby

Blowby is defined as the gas that flows from the combustion chamber into the crankcase. The flow is mainly through the ring gaps. In a well maintained engine the blowby flow accounts for about 1% of the total flow. The gases that ends up in the crankcase are ventilated back to the intake which will affect the properties in the intake systems. Earlier the gases that ended up in the crankcase were ventilated directly to the atmosphere and accounted for a significant source of HC emissons (Heywood, 2019).

2.7 Heat Transfer

Heat transfer can occur due to convection, conduction and radiation. In engines the main heat transfer is from convection. Convection is the mode of heat transfer

between a solid surface and the adjacent liquid or gas that is in motion (Cengel et al., 2017). In CI engines there is also a contribution in the heat transfer from radiation (Eriksson and Nielsen, 2014), which has been neglected in this thesis. Radiation is that energy is emitted by electromagnetic waves or photons as a result of change in the electrons configuration (Cengel et al., 2017). The heat transfer due to convection from gas to cylinder wall is calculated using Newton's law of cooling:

$$\dot{Q}_{HT} = hA\Delta T = hA(T - T_w) \tag{2.43}$$

h is the convection heat transfer coefficient and is not a property of the fluid. It is an experimentally determined parameter whose value depends on all parameters influencing convection.

2.8 Combustion

The combustion in CI engines starts when the injected fuel ignites. It is characterized by three phases; ignition delay, premixed combustion and mixing controlled combustion.

2.8.1 Ignition Delay

Before the actual combustion starts in CI engines the fuel is transformed from a cold liquid to a vapor and reach a sufficient temperature to autoignite. The time it takes from SOI (start of injection) until the fuel autoignites is the ignition delay. This delay is not present in SI engines since the combustion starts when the fuel is ignited by a spark from the spark plugs.

There have been attempts to use experimental correlations to determine the igntion delay in CI engines. Traditionally Arrhenius correlations have been used, where A and n are tuning constants and E_A is the activation energy for the reaction:

$$\tau_{id} = Ap^{-n}\exp\left(\frac{E_A}{\bar{R}T}\right) \tag{2.44}$$

Heywood (2019) suggests that the Arrhenius correlations does not seem useful according to several reasons, one is that it is a to simple expression to represent the overall complex chemistry involved.

Another empirical formula developed by Hardenberg and Hase (1979) for predicting the ignition delay in CI-engines has shown resonable agreement with experimental data from different engine conditions (Heywood, 2019) :

$$\tau_{id}(CA) = (0.36 + 0.22\bar{S}_p)\exp\left(E_A\left(\frac{1}{\bar{R}T} - \frac{1}{17.190}\right) + \left(\frac{21.2}{p - 12.4}\right)^{0.63}\right) \tag{2.45}$$

the cylinder pressure p in this equation is given in [bar].

The apparent activation energy E_A is given by

$$E_A = \frac{618.840}{CN + 25} \tag{2.46}$$

where CN is the fuel cetane number. The cetane number is a measure on the fuels ability to resist autoignition (Heywood, 2019).

2.9 Combustion Modelling

The combustion has in this thesis used a single s-shaped Vibe function according to equation (2.47).

$$x_b(\theta) = \begin{cases} 0, \theta < \theta_{SOC} \\ 1 - e^{-a\left(\frac{\theta - \theta_{SOC}}{\Delta\theta}\right)^{m+1}}, \theta \geq \theta_{SOC} \end{cases} \tag{2.47}$$

In the Vibe functions $\Delta\theta$ and a are related to the combustion duration and m affects the shape of the Vibe, θ_{SOC} denotes the start of combustion. The Vibe function starts at 0 and goes to 1.

The derivative of the Vibe function with respect to θ is:

$$\frac{dx_b(\theta)}{d\theta} = \frac{a(m+1)}{\Delta\theta}\left(\frac{\theta - \theta_{soc}}{\Delta\theta}\right)^m e^{-a\left(\frac{\theta - \theta_{SOC}}{\Delta\theta}\right)^{m+1}} \tag{2.48}$$

The combustion duration used in the Vibe function used the following rule of thumb $\Delta\theta = \Delta\theta_d + \Delta\theta_b$ (Eriksson and Nielsen, 2014). The parameter m has been assigned a value and θ_{SOC} is taken when the MFB trace reaches a small value. The parameter a has been optimized from MFB trace with the parameters discussed above used in the Vibe function. The optimization have been performed with `lsqcurvefit` in Matlab.

$$\min_x \|F(x) - y\|_2^2 = \min_x \sum_i (F(x_i) - y_i)^2 \tag{2.49}$$

`lsqcurvefit` solves nonlinear curve-fitting problem in a least-squares sense as described in equation (2.49). $F(x)$ denotes the value from the function and y denotes observed values. The function minimizes the squared difference between the function and the observed values.

The combustion in CI engines with single injection has two phases, a premix and a main burning. This is often modeled by the sum of two Vibe functions (Eriksson and Nielsen, 2014).

A simple model that describes the combustion efficiency is discussed in Eriksson and Nielsen (2014, p 72):

$$\eta_{co} = \min(1, \lambda) \tag{2.50}$$

However in CI applications the mixture will be lean meaning $\lambda \geq 1$ and it is therefore a good approximation to assume that all fuel is burnt. η_{co} will vary in SI-engines due to that the mixture is sometimes rich meaning $\lambda < 1$.

The heat release from combustion can then be calculated:

$$\begin{aligned} \frac{dQ_{HR}(\theta)}{d\theta} &= m_f Q_{LHV} \eta_{co} \frac{dx_b(\theta)}{d\theta} \\ &\overbrace{=}^{\text{Eq:(2.50)}} m_f Q_{LHV} \frac{dx_b(\theta)}{d\theta} \end{aligned} \tag{2.51}$$

The heat release dependent on time is obtained from the following:

$$\frac{dQ_{HR}}{dt} = \frac{dQ_{HR}(\theta)}{d\theta} \omega_e \tag{2.52}$$

2.10 Heat Release Analysis

The MFB trace can be provided from a heat release analysis. The subchapters describes different methods to retrive the heat release from cylinder pressure data. It is common to take out the CA values when MFB is 10 %, 50 % and 90 %. To denote these CA the following notation is used $CA_{x,10}$, $CA_{x,50}$ and $CA_{x,90}$. From these CA a set of definitions are made:

Flame development angle $\Delta\theta_d$ - It is the CA-interval from SOC until $CA_{x,10}$.
Rapid burning angle $\Delta\theta_b$ - It is the CA-interval from $CA_{x,10}$ until $CA_{x,90}$.
MFB 50 - It is the angle $CA_{x,50}$ and it is often used as an indicator of the combustion position.

2.10.1 Net Heat Release Analysis

A common way to decide the mass fraction burned from cylinder pressure data is to use the net heat release. That method was originally presented in Krieger and Borman (1966), however the equation here is taken from Eriksson and Nielsen (2014).

The heat release rate is the following:

$$\frac{dQ_{net}}{d\theta} = \frac{V(\theta)}{\gamma - 1} \frac{dp(\theta)}{d\theta} + \frac{\gamma}{\gamma - 1} p(\theta) \frac{dV(\theta)}{d\theta} \tag{2.53}$$

In this method a constant γ is used, in reality that is not completly true because γ changes with temperature and gas composition. This model does not consider the

fact that there is heat transfer which will affect the pressure curve. The net heat release method requires the derivative of the cylinder pressure. This means that noise needs to be removed from the data set in order to achieve good results. It is important to use non-causal filtering techniques in order to prevent phase shift of the filtered cylinder pressure data. The pressure derivative can be estimated with:

$$\frac{dp(\theta)}{d\theta} = \frac{p(\theta_{i+1}) - p(\theta_{i-1})}{\theta_{i+1} - \theta_{i-1}} \tag{2.54}$$

The heat release is finally given by the following equation

$$Q_{net}(\theta) = \int_{\theta_{ivc}}^{\theta} \frac{dQ_{net}(\alpha)}{d\alpha} d\alpha \tag{2.55}$$

To get the MFB an assumption that it is proportional to the net heat release gives the following expression

$$x_b(\theta) = \frac{Q_{net}(\theta)}{\max(Q_{net}(\theta))}. \tag{2.56}$$

2.10.2 Rassweiler and Withrow's Method

Rassweiler and Withrow's method is the classical way of estimating the MFB. The method was originally presented in Rassweiler and Withrow (1938), however the equations used here are taken from Eriksson and Nielsen (2014). The method builds on the knowledge that when there is no combustion the cylinder pressure can be represented well with a polytropic relation

$$pV^{\kappa} = \text{constant} \tag{2.57}$$

The pressure change between two samples is

$$\Delta p = p_{i+1} - p_i \tag{2.58}$$

The pressure change is assumed to be made up of the pressure raise from combustion, Δp_c and pressure raise due to volume change, Δp_v,

$$\Delta p = \Delta p_c + \Delta p_v \tag{2.59}$$

The pressure and volumes between samples when there is no combustion are related as

$$p_i V_i^{\kappa} = \hat{p}_{i+1} V_{i+1}^{\kappa} \tag{2.60}$$

This leads to the following expression

$$\Delta p_v = \hat{p}_{i+1} - p_i = p_i \left(\left(\frac{V_i}{V_{i+1}} \right)^{\kappa} - 1 \right) \tag{2.61}$$

Now the pressure due to combustion can be extracted from equation (2.59). Assuming that the pressure raise due to combustion is propotional to the MFB.

$$x_b(i) = \frac{m_b(i)}{m_b(\text{total})} = \frac{\sum_0^i \Delta p_c}{\sum_0^M \Delta p_c} = \frac{\sum_0^i \Delta p - \Delta p_v}{\sum_0^M \Delta p - \Delta p_v} \tag{2.62}$$

In the equation above M denotes the total number of crank angle intervals.

2.11 Mass Fraction Burned

The MFB is obtained from cylinder pressure by Matekunas Pressure Ratio. The MFB is used to determine the parameters for the single Vibe function.

2.11.1 Matekunas Pressure Ratio

The MFB is obtained from the cylinder pressure by using Matekunas Pressure ratio. The pressure ratio concept is computationally efficient and it can be used to determine an approximation of the MFB. The pressure ratio is defined as the ratio of cylinder pressure from a fired cycle $p(\theta)$ and the pressure from a motored cycle $p_m(\theta)$:

$$PR(\theta) = \frac{p(\theta)}{p_m(\theta)} - 1. \tag{2.63}$$

The pressure ratio is then normalized by its maximum to produce heat release traces similar to MFB.

$$PR_N(\theta) = \frac{PR(\theta)}{\max(PR(\theta))}. \tag{2.64}$$

Klein (2007) explains that investigastions have shown that Matekunas pressure ratio gets $PR_N(\theta) = 0.5$ in the order of 1-2 degrees from $CA_{x,50}$. That suggests that the pressure ratio concept is suitable for estimating the MFB trace.

2.11.2 Polytrope

In Matekunas pressure ratio the motored pressure $p_m(\theta)$ is used. To get an estimation of the motored pressure the polytropic exponent is fitted to measured cylinder pressure. The optimization of the exponent is performed on the pressure

trace from IVC and 20 CA forward. That gives sufficient data to optimize the polytropic exponent κ. The compression part in the four strokes are well modelled with a polytrope according as in the following equation

$$pV^{\kappa} = constant. \tag{2.65}$$

Since the constant in the polytrope is the same for different pressures and volumes on the polytrope curve the following relation is derived

$$p_{init}V_{init}^{\kappa} = p(\theta)V(\theta)^{\kappa} \tag{2.66}$$

$$\frac{p_{init}}{p(\theta)} = \left(\frac{V(\theta)}{V_{init}}\right)^{\kappa} \tag{2.67}$$

$$\log\left(\frac{p_{init}}{p(\theta)}\right) = \kappa \log\left(\frac{V(\theta)}{V_{init}}\right) \tag{2.68}$$

Least squares have been used on the last equation to give the optimal κ in a least squares sence to measured cylinder pressure.

In Figure 2.6 the polytrope fitted to a fired pressure trace is shown. The measured pressure is reaching a larger value than the maximum pressure from the polytropic compression the larger value is due to combustion.

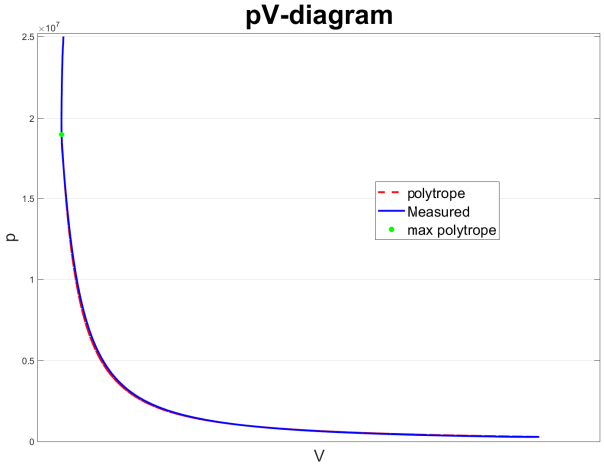

Figure 2.6: *Polytrope fitted to a pressure curve.*

2.12 Analytic Pressure Model

The analytic pressure model was originally presented in Eriksson and Andersson (2002) however it has been further developed in Eriksson and Nielsen (2014,

Ch 7.8). Note that the model described is intended for SI-engines therefore modifications are needed to fit CI-engines. Model assumptions for the In-cylinder pressure model:

- The compression is modeled as a polytropic process with a correctly chosen exponent means the compression with heat transfer can be well approximated.
- Similarly the expansion process can be described by a polytropic process. Providing a reference point for expansion temperature and pressure which is calculated using constant-pressure combustion process.
- The pressure ratio is similar to the mass fraction burned profile which is modeled by a Vibe function see equation (2.47).
- The gas exchange is treated as that the pressure during intake is said to be the same as the intake manifold pressure. During the exhaust stroke the pressure is modeled as the pressure in the exhaust manifold. During valve overlap the pressure can be determined by interpolating a sine function.

3
Modelling

This chapter describes the models that have been used in the cylinder model. The temperature and pressure are modeled by the temperature and pressure states described in Chapter 2. The instantenous volume is calculated based on engine geometry.

3.1 Gas Flows

Figure 3.1 shows some important parameters of the poppet valve geometry. These parameters are used to determine discharge coefficient C_D from look up tables and to calculate the effective flow area A_E from refrence area and discharge coefficient.

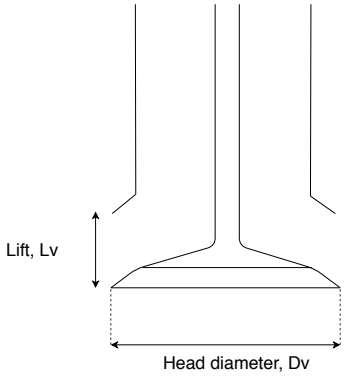

Figure 3.1: *Poppet valve geometry.*

The flow through the valves have been modeled as compressible flow. Discharge coefficients C_D have been measured in an air flow bench. The discharge coefficient for the intake valve depends on the intake valve lift $L_{v,intake}$.

$$C_{D,intake} = f_{lookup}(L_{v,intake}(\theta)) \tag{3.1}$$

The discharge coefficient for the exhaust valve depends on the exhaust valve lift $L_{v,exhaust}$ and the pressure ratio $Pr = \frac{p_{cyl}}{p_{em}}$ between cylinder pressure p_{cyl} and the pressure in the exhaust manifold p_{em}.

$$C_{D,exhaust} = f_{lookup}(L_{v,exhaust}(\theta), Pr) \tag{3.2}$$

L_v denotes the valve lift which is assumed to be the same for all cases even though when the pressure ratios are much higher, leading to large forces, which will alter the lift profile. A figure of the lift profiles for intake, exhaust and CRB is shown in Figure A.1. The C_D values for intake valve and exhaust valve are shown in Figures A.2 and A.3.

The effective flow area in the compressible flow equation is for exhaust and intake valve given by the product of the discharge coefficient C_D and the reference area A_R.

$$A_E = C_D \underbrace{\frac{D_v^2 \pi}{4}}_{A_R}. \tag{3.3}$$

CRB uses the same C_D lookup as for the exhaust valve since it is the exhaust valve that is opened. However when the exhaust is blown out there are two exhaust valves that are open while with CRB there is only one valve that is opened. In the air flow bench C_D has been measured for one valve therfore a scaling of 2 is performed on the effective area A_E for the intake and exhaust valve. For the CRB case there is no scaling of the effective area since only one valve is opened, however CRB have another valve lift $L_{V,CRB}$ which is completly different from the exhaust valve lift, see Figure A.1. The CRB lift has the same phase compared to the exhaust lift however the exhaust lift and intake lift can be phased individually. A function has been implemented that looks how much the intake and exhaust have been phased. The function then translates the crank angle to fit the original valve lift in Figure A.1, this is performed to ensure that the valves in the simulation opens at the correct CA.

3.1.1 Oscillating Mass Flow

The simulated mass flow had oscillations. This was dealt with by including a linear region for the compressible flow, see Equation (2.42). In Figure 3.2 the mass flow is shown before the linear region was added. The size of the region

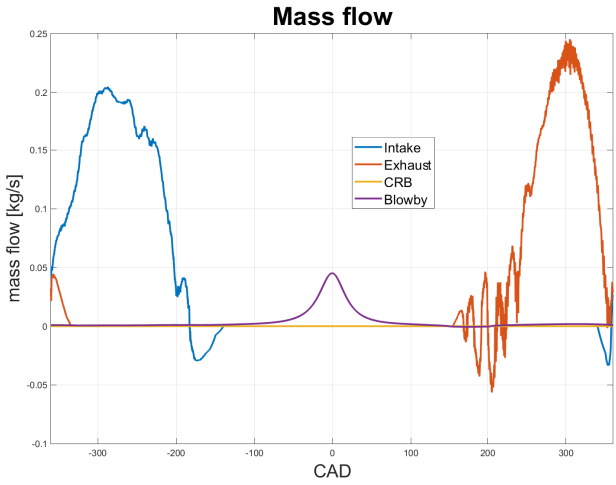

Figure 3.2: *Oscillating mass flow, without linear region in* Ψ.

was tested until the oscillations disappeared. The intention of adding the linear region is to achieve simulation stability.

Figure 3.3 shows the massflow after the linear region was added. The oscillations at 200 CAD have decreased.

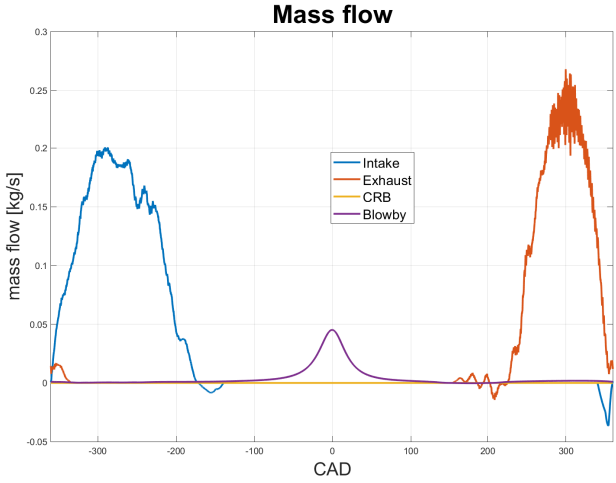

Figure 3.3: *Mass flow, linear region included in* Ψ.

3.1.2 Blowby Flow

The blowby flow has been modeled as a compressible flow. In this thesis there where no discharge coefficients measured for the blowby flow. Instead the effective area A_E was used as a tuning parameter to get a good match with measured pressure curve. Measurements at Scania have shown that the blowby flow is affected by the temperature in the cylinder. The ring gap between piston ring and cylinder wall gets smaller when the temperature increases and that affects the effective area in the flow equation. The temperature and pressure in the crankcase used in the compressible flow equation are set as ambient temperature and pressure.

3.2 Gas Properties

The working fluid is the simplified air model discussed in equation (2.20) for the motored pressure and VVB. The gas properties have been obtained from the NASA polynomials. Figure 3.4 shows simulated temperature in the cylinder at high load. It shows that the temperature is well within the interval for the common species in NASA polynomials wich is up to 5000 K.

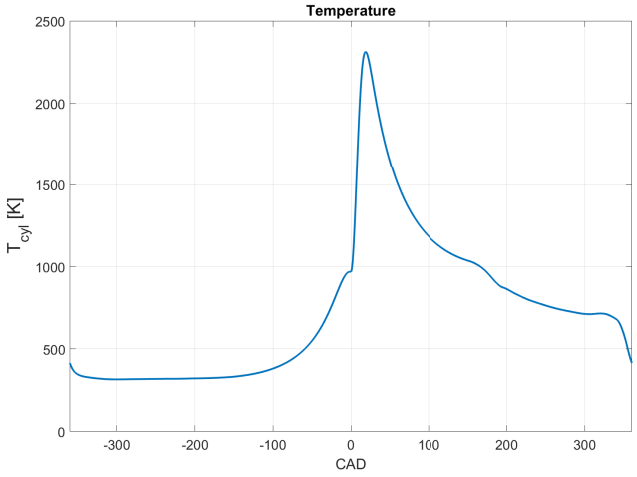

Figure 3.4: *Simulated temperature in the cylinder at full load.*

Heywood (2019) concludes that the peak burned gas temperature in ICE is of order 2500 K which is in accordance with the simulated temperature presented in Figure 3.4.

3.2.1 Combustion Gas Properties

During combustion the gas properties are also affected by burned gases and a state is used to keep track of the mass fraction of air x_{air}. The mass fraction of burned gases is $x_{burned} = 1 - x_{air}$. An assumption made is that the fuel used is cetane $C_{16}H_{34}$ wich has lower heating value $Q_{LHV} = 44\,\text{MJ/kg}$ and the stochiometric air/fuel ratio $(A/F)_s = 14.8$ (Eriksson and Nielsen, 2014).

To be able to model the combustion an assumption is that the combustion is between air and hydrocarbons. The chemical reaction is thus the following:

$$n_{fuel}\underbrace{C_aH_b}_{\text{Fuel}} + n_{air}\underbrace{(O_2 + 3.773N_2)}_{\text{Air}} + n_{Burned}\underbrace{\left(aCO_2 + \frac{b}{2}H_2O + 3.773\left(a + \frac{b}{4}\right)N_2\right)}_{\text{Burned}} \longrightarrow$$
$$\left(n_{fuel} + n_{Burned}\right)\underbrace{\left(aCO_2 + \frac{b}{2}H_2O + 3.773\left(a + \frac{b}{4}\right)N_2\right)}_{\text{Burned}} +$$
$$+\left(n_{air} - n_{fuel}\left(a + \frac{b}{4}\right)\right)\underbrace{(O_2 + 3.773N_2)}_{\text{Air}} \tag{3.4}$$

The number of moles that is involved in the reaction is calculated at IVC.

$$n_{tot,air} = 1 + 3.773 \tag{3.5}$$

$$n_{tot,Burned} = a + \frac{b}{2} + 3.773 \tag{3.6}$$

$$n_{air} = \frac{m_{IVC}x_{air}}{M_{air}n_{tot,air}} \tag{3.7}$$

$$n_{fuel} = \frac{m_{fuel}}{M_{fuel}} \tag{3.8}$$

$$n_{Burned} = \frac{(1 - x_{air})m_{IVC}}{M_{Burned}n_{tot,Burned}} \tag{3.9}$$

In the equations above m_{IVC} denotes the mass in the cylinder at IVC.

x_{air} is modeled as a state

$$\frac{dx_{air}}{dt} = \underbrace{\frac{RT}{pV}}_{\frac{1}{m}}\sum_i (x_{air,i} - x_{air})\dot{m}_i - C\frac{dx_b}{dt} \tag{3.10}$$

$\frac{dx_b}{dt}$ correspond to the derivative of the Vibe function and C is a scaling of the Vibe function to make sure that after the combustion the mass fraction of air is according to what is predicted in equation (3.4).

In the equation above the sum corresponds to the filling and emptying of the cylinder. With $x_{air,intake} = 1$ it is assumed that no residual gases are present in the intake since the engine does not have EGR. It is only the filling of the cylinder and the combustion that affect the state, since it is assumed that the compostion in the cylinder is homogeneous. The idea to model the mass fraction has been used in Wahlström and Eriksson (2011) where they kept track of the mass fraction of oxygen x_{O_2}. If the flow goes from the cylinder to the intake manifold the state x_{air} is not altered since it is only the filling of the cylinder and combustion that alters the state.

The molar fraction of x_{air} after the combustion, (here it is assumed that the combustion efficiency $\eta_{lco} = 1$ since CI engines runs lean).

$$\tilde{x}_{air,afterCombustion} = \frac{\left(n_{air} - n_{fuel}\left(a + \frac{b}{4}\right)\right) n_{tot,air}}{\left(n_{air} - n_{fuel}\left(a + \frac{b}{4}\right)\right) n_{tot,air} + \left(n_{Burned} + n_{fuel}\right) n_{tot,Burned}} \tag{3.11}$$

Finally the mass fraction of air after combustion is calculated:

$$x_{air,afterCombustion} = \frac{\tilde{x}_{air} M_{air}}{(1 - \tilde{x}_{air}) M_{\text{Burned}} + \tilde{x}_{air} M_{air}} \tag{3.12}$$

The scaling of the Vibe function is thus:

$$C = x_{air,beforeCombustion} - x_{air,afterCombustion} \tag{3.13}$$

The gas mass specific gas constant has been calculated as

$$R = (1 - x_{air}) R_{Burned} + x_{air} R_{air} \tag{3.14}$$

The mass specific heat at constant pressure have been calculated as

$$c_p = (1 - x_{air}) c_{p,Burned} + x_{air} c_{p,air} \tag{3.15}$$

where $c_{p,air}$ and $c_{p,Burned}$ have been obtained from the NASA polynomials and Equation (2.24b).

From the ideal gas assumption c_v is obtained as

$$c_v = c_p - R \tag{3.16}$$

Figure 3.5 shows how the mass fraction of air changes at full load 2500 Nm when $\lambda = 1$. The mass fraction of air goes to 0 which is what is expected since at $\lambda = 1$ the only products from the reaction is N_2, CO_2 and H_2O meaning that all oxygen O_2 is consumed.

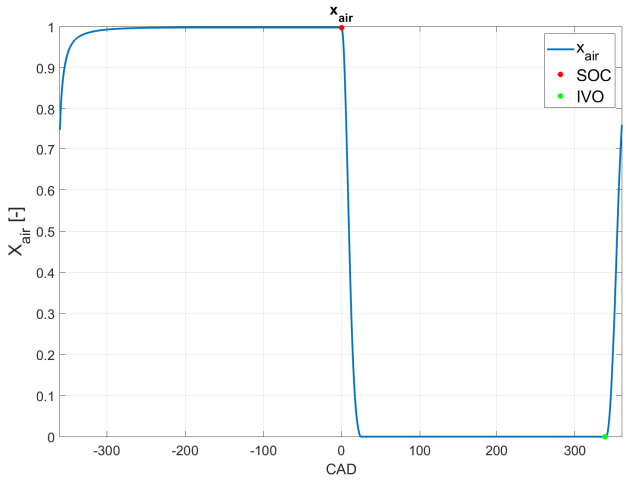

Figure 3.5: *Mass fraction air at full load when* $\lambda = 1$.

3.3 Heat Transfer

The empirical formula used to describe the convection heat transfer coefficient in the cylinder is described in Chapter 3.3.1.

The cylinder wall tempreature T_w is for a fully warmed up engine 140°C according to Guzzella and Onder (2010, p 335). That is the wall temperature that has been used in equation (2.43). In equation (2.43) it is assumed that the temperature is homogeneous in the entire combustion chamber. Equation (2.7) calculates the instantaneous area of the combustion chamber depending on θ. It has here been assumed that the combustion chamber is a perfect cylinder. The wall temperature in the cylinder will have lower temperature than the piston crown, however a simplification made is that the temperature is the same for piston crown and the cylinder walls.

3.3.1 Woschni

A method to calculate the heat transfer coefficient was originally presented in Woschni (1967), however equation (3.17) is taken from Eriksson and Nielsen (2014):

$$h = C_0 B^{-0.2} p^{0.8} w^{0.8} T^{-0.53} \tag{3.17}$$

with $C_0 = 1.30 \cdot 10^{-2}$.

The characteristic velocity in equation (3.17) is given by the following expression:

$$w = C_1 \bar{S}_p + C_2 \frac{V T_{ivc}}{V_{ivc} p_{ivc}} (p - p_m) \tag{3.18}$$

The expression only depends on the mean piston speed when there is no combustion. The motored pressure and the cylinder pressure is in that case the same. The mean piston speed is given from engine geometry and kinematics as the following:

$$\bar{S}_p = \frac{2aN_e}{60} \tag{3.19}$$

Table 3.1 describes how the constants in Woschni's model change during the different strokes in the four stroke cycle.

Table 3.1: *Constants used in Woschni's model.*

	Gas Exchange	**Compression**	**Combustion and expansion**
C_1	6.18	2.28	2.28
C_2	0	0	0.00324

The motored pressure is modelled well with a polytrope, κ is the polytropic exponent.

$$p_m(\theta) = \begin{cases} p(\theta), \theta \leq \theta_{SOC} \\ p(\theta_{SOC}) \left(\frac{V(\theta_{SOC})}{V(\theta)} \right)^{\kappa}, \theta > \theta_{SOC} \end{cases} \tag{3.20}$$

For $p_m(\theta)$ in Woschni the polytropic exponent κ have been assigned to a constant value. The value on κ was optimized from a motored cycle. This is because the model should be as generic as possible and require as few calibrations as possible for different engine loads. Another way would be to use measured motored pressure from an engine test cell as $p_m(\theta)$ in equation (3.18).

3.4 Torque Model

A simple instanteneous engine torque model that neglects friction is presented in Eriksson and Nielsen (2014) and it is the following

$$M_{e,i}(\theta) = \sum_{j=1}^{n_{cyl}} (p_{cyl,j}(\theta - \theta_j^0) - p_{amb}) AL(\theta - \theta_j^0). \tag{3.21}$$

θ_j^0 denotes the individual offset of each cylinder. The pressure in the crank case is set to the ambient pressure $p_{amb} = 1$ [bar]. Note that the product of the area

and the crank lever is the same as the volume derivative with respect to crank angle see Equation (2.5).

$$AL(\theta) = \frac{dV}{d\theta} = \frac{dV}{dt}\frac{1}{\omega_e} \tag{3.22}$$

The average torque obtained from the four strokes is of interest in for example the gearbox. A formula for calculating the average torque is the following:

$$M_e = \frac{1}{4\pi}\int_0^{4\pi} M_{e,i}(\theta)d\theta - M_f \tag{3.23}$$

M_f denotes friction, which has been neglected in this thesis. The calculations from the torque model have been performed from simulation on one cylinder.

4

Data acquisition

This chapter describes the placement of the sensors used to acquire data and what type of measurement equipment that has been used to collect the data. There will also be a discussion on the physical principle of piezoelectric sensors and how to deal with the problem of not knowing the absolute cylinder pressure from the cylinder pressure sensor. The data has been collected in an engine test cell at Scania CV AB. The measurements have been conducted at steady-state conditions.

The measured cylinder pressure is crank angle resolved, however it needs an absolute level on the pressure at some point in a cycle. Methods for that are described in chapter 4.1. The manifold pressures are crank angle resolved, it is necessary due to the fact that the pressure varies during the cycle. Pressure variations in the intake and exhaust manifolds are due to pulsations caused by the opening and closing of valves. The temperatures in the manifolds are averaged on all sensors during one cycle.

The measurements have been collected from an inline 6 cylinder Scania prototype engine with VVT and CRB. The cylinder pressure has been measured in cylinder 6 because it is the cylinder that is the closest to the flywheel. There the torsion and crankshaft flexibility is the smallest and hence neglected. The pressure in the intake manifold has been measured close to the inlet valve of cylinder 6. The pressure in the exhaust manifold has been collected close to the exhaust valve of cylinder 6. Figure 4.1 shows a simplified sketch of the location of the various sensors. Measurements have also been performed on cylinder 1 but those have not been used in the cylinder model.

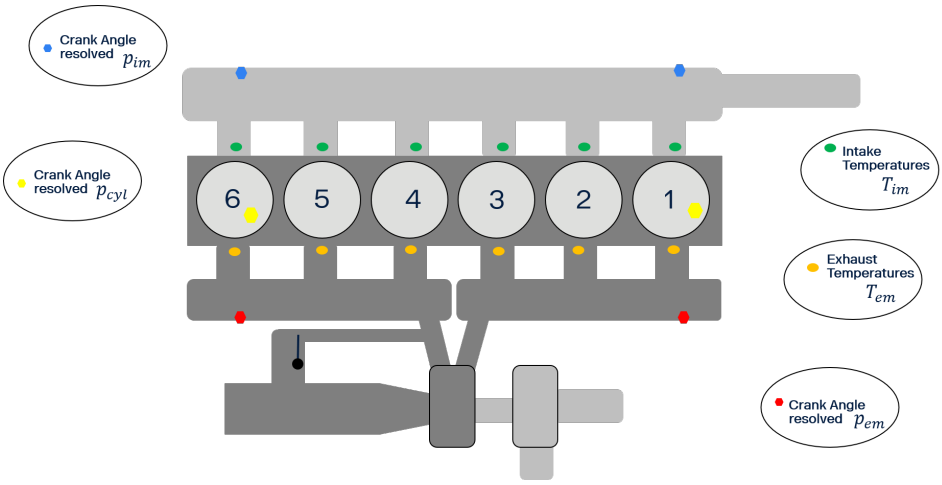

Figure 4.1: *An overview of the engine and its sensor locations.*

Table 4.1: *Description of measured signals used for input to the Simulink model in this thesis.*

Symbol	Description	Unit
I_{phase}	Phasing of IVO and IVC.	[CA]
E_{phase}	Phasing of EVO and EVC.	[CA]
m_f	Mass of fuel injected	[kg]
N_e	Engine speed	[RPM]
$p_{im}(CAD)$	Intake manifold pressure	[Pa]
$p_{em}(CAD)$	Exhaust manifold pressure	[Pa]
SOI	Start of injection	[CA]
T_{im}	Intake manifold temperature	[K]
T_{em}	Exhaust manifold temperature	[K]

Table 4.2 describes the outputs from the Simulink model implemented in this thesis.

Table 4.2: *Outputs from the Simulink model.*

Symbol	Description
$\frac{dT}{dt}$	Temperature state.
$\frac{dp}{dt}$	Pressure state.
m	Mass in the cylinder.
$\frac{dx_{air}}{dt}$	Mass fraction of air state.
M_{ei}	Instantenous torque.
Φ_{cyl}	Φ in the cylinder at IVC.

Table 4.3 presents signals used for evaluating the Simulink model. p_{cyl} is the measured cylinder pressure. λ_{af} is evaluated from measurment of massflow of air and fuel and it is assumed that the fuel is known to be able to obtain the stochimoetric $(A/F)_s$ value. $M_{flywheel}$ is the averaged torque measured at the flywheel.

Table 4.3: *Description of signals used for evaluation.*

Symbol	Description	Unit
$p_{cyl}(CAD)$	Cylinder pressure	[Pa]
λ_{af}	Lambda	[-]
$M_{flywheel}$	Measured torque at the flywheel	[Nm]

4.1 Absolute Reference Of Cylinder Pressure

The cylinder pressure is measured by a piezoelectric transducer. By design the transducer responds to pressure differences by outputting a charge reference to an arbitrary ground. This means that the transducer at some point must be directly correlated to pressure (Randolph, 1990). To get a useful signal from the measurements a charge amplifier is needed. The charge amplifier is adjusted so that a useful signal can be obtained. The adjustment is done so that the leakage current is small. The signal from the amplifier decreases exponentially. That can be used to reconstruct the true pressure curve. The knowledge that the derivative of an exponential is the same as the function itself means that the rate of which the signal decreases is propotional to the signal level. The signal from the charge amplifier measures relative change of the cylinder pressure well but not the absolute value of the cylinder pressure (Johansson, 2003). In Johansson (2003) diffrent ways of chosing the absolute value for the cylinder pressure is discussed:

1. Set the cylinder pressure equal to the pressure in the intake manifold at BDC.
2. Set the cylinder pressure during the exhaust stroke equal to exhaust backpressure.
3. Assume polytropic compression with known κ.
4. Assume polytropic compression with unknown κ.

The methods described in Johansson (2003) was evaluated in Randolph (1990), there they concluded that the best method was pegging at BDC. The method worked best in untuned intake systems or at low speed in tuned systems. Tuned systems means that the pulsating pressure waves from the exhaust system is appropretly arranged so that the wave will raise the nominal inlet pressure which will increase induced air in to the cylinder (Heywood, 2019). The uncertainty of using only one sample when pegging at BDC is removed by taking one sample before BDC and one after to avoid error from point measurements.

5

Result and Discussion

The figures in this chapter will compare simulated results with cycle averaged results from measurements. In Figure 5.1 a pressure curve from a high load case is presented. As seen in the figure the pressure curve does not change much from one cycle to another. Thereby a representative pressure curve is to average all pressure curves and compare the simulated pressure to that pressure curve. All figures in this Chapter that have CAD at the x-axis are plotted in the interval ±360 CAD, where 0 CAD corresponds to TDC fire. The measurments used to validate the results have been measured at stationarity.

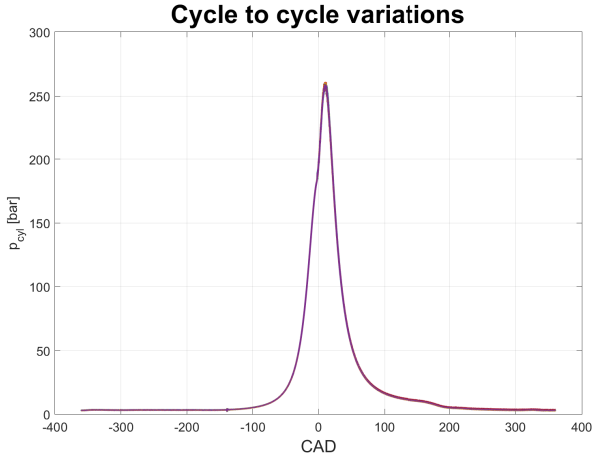

Figure 5.1: *Pressure plot for 50 consecutive cycles at high load.*

5.1 Motored Pressure

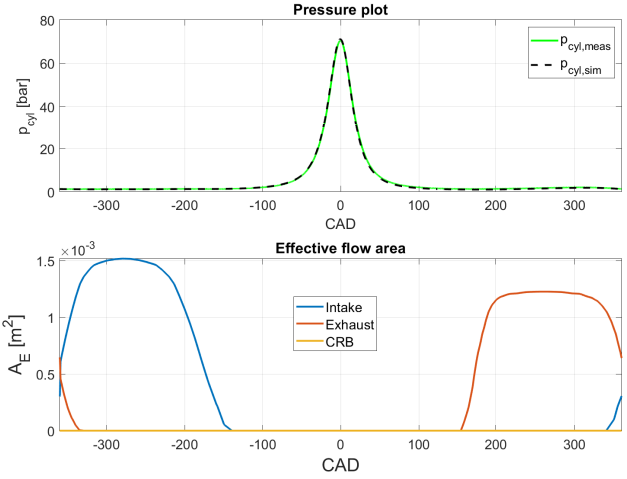

Figure 5.2: *CAD pressure plot and effective valve flow area at 1400 RPM.*

In the motored measurements the fuel have been cut off and an electric motor have cranked the engine. Figure 5.2 shows the CAD pressure plot at 1400 RPM and the effective flow area A_E for the intake and exhaust valve. In this case IVO and EVO are the standard values and there is no phasing of the valves. The simulated pressure shows good agreement with the measured pressure see, Figures 5.2 and 5.3.

Figure 5.3 shows the pV-diagram for the motored case. In Figure 5.3 it is seen that the simulated pressure has a larger peak than the measured. The reason can be that there are production tolerances in the compression ratio r_c. The compression polytrope deviates from the measured as do the expansion polytrope. The reason is most likely that the heat transfer model fails to model the true heat transfer in the cylinder. The temperature is the same for cylinder wall and piston which is a potential source of error. Measurments at Scania have shown that the piston is warmer compared to the cylinder walls. That in turn will affect the size of the ring gap which will affect the effective flow area for the blowby flow. The average indicated torque predicted by the simulink model is -146 Nm. The averaged measured torque at the flywheel was -161 Nm. The reason for the difference is most likely that the torque model neglects friction and that the pV-diagram are not exactly identical. Measured torque also includes friction and hence should be slightly more negative.

Figure 5.4 shows the simulated massflows. The blowby flow is biggest at TDC since the effective flow area is set as a small constant and that the cylinder pressure is largest at TDC for motored cycles. As expected the flow from the

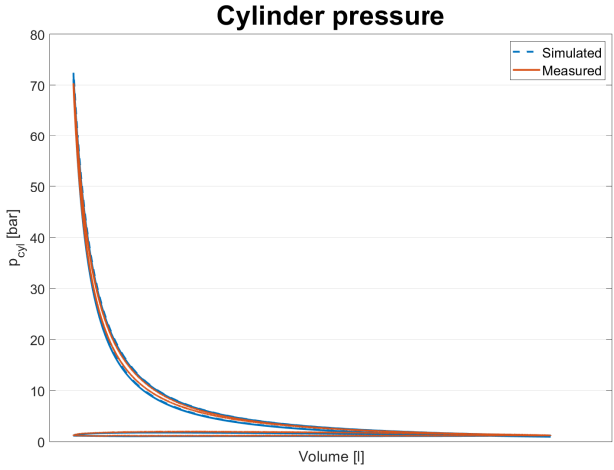

Figure 5.3: *pV diagram for motored pressure at 1400 RPM*

intake manifold is most of the time into the cylinder but there is however backflow to the intake manifold. Note that positive flow is taken as the definition in Figure 2.3. It is into the cylinder for the intake valves and out of the cylinder for the exhaust valves.

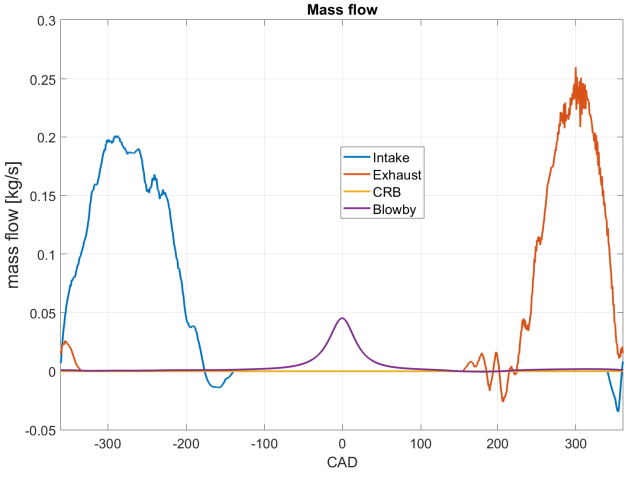

Figure 5.4: *Simulated massflow motored cycle at 1400 RPM.*

Figure 5.5 is a motored cycle at 1500 RPM where the intake and exhaust valves

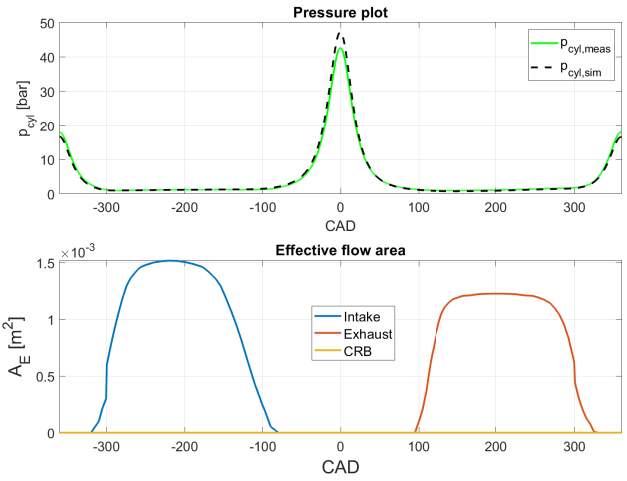

Figure 5.5: *CAD pressure plot and effective flow area at 1500 RPM symmetrically phased. Intake is phased 60 ° and exhaust is phased -60 °.*

have been symmetrically phased by 60 ° and -60 ° respectively. It is seen that the model captures the physics quite well but the maximum pressure deviates somewhat from the measured. The simulated pressure peak at 0 CAD is too high while the peaks at ± 360 are too low. A reason might be that the measurments from the cylinder pressure sensor is pegged at BDC once each cycle. Other reasons might be that the valve lift might deviate somewhat from what is presented to the model see Figure A.1. That can be due to production tolerances or ageing of the material. The valve lifts have been measured when the valve is cold. During operation the valve gets warmer and the valve gets longer and thereby it alters the duration and when the actual IVO and EVO occurs which will affect the result especially at full loads.

In Figure 5.6 it is seen that the compression and expansion polytropes deviates from the measured. The reason for that is most likely that the heat transfer in this case is too high. A better result could probably be achieved with a lower wall temperature T_w. The simulated average indicated torque is -112.1 Nm and the measured including friction, is -128.6 Nm. Figure 5.7 shows the simulated massflow and compared to Figure 5.4 there is much more backflow meaning that the mass in the cylinder will be less. Thereby it is resonable that the peak pressure is lower for the case when symetrical phasing has been used.

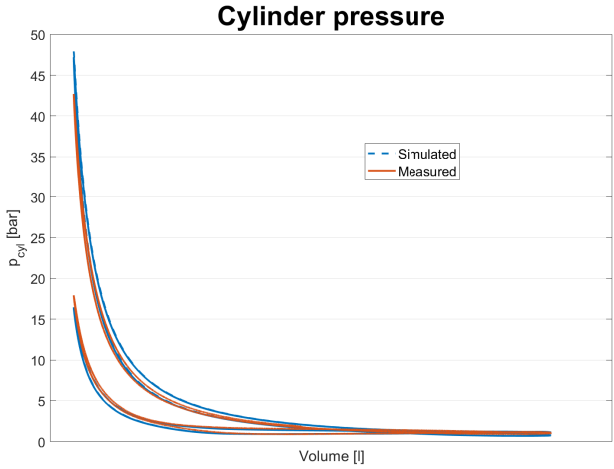

Figure 5.6: *pV diagram for symmetrically phased 60° at 1500 RPM. Intake is phased 60 ° and exhaust is phased -60 °.*

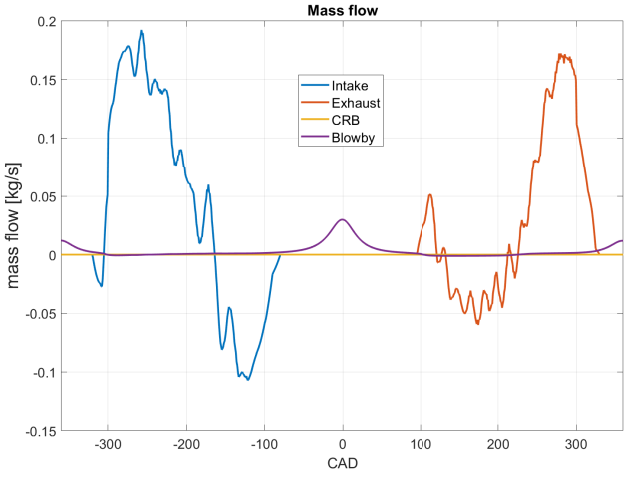

Figure 5.7: *Simulated massflow for symmetrically phased 60° at 1500 RPM. Intake is phased 60 ° and exhaust is phased -60 °.*

5.2 CRB

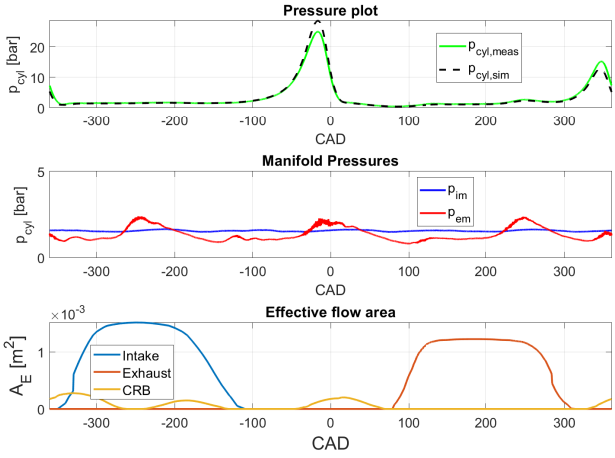

Figure 5.8: *Pressure CAD plot CRB 1000 RPM. The manifold pressures for intake and exhaust are seen. The intake manifold pressure is rather constant while the exhaust manifold pressure have pulses. The effective flow area shows that the CRB is activated.*

This subchapter will discuss results from simulation compared to measured cylinder pressure when CRB have been used. In Figures 5.8, 5.11, 5.10 and 5.13 it is seen that CRB lift is also activated. In those Figures it is also seen that the CRB valve is open at the point where the cylinder pressure has its peaks. The pressure ratios between exhaust manifold and cylinder pressure is well above 5.5, seen in Figures 5.8 and 5.11. That is the maximum pressure ratio that has been measured for the C_D values for the exhaust valve, see Figure A.3. Another uncertainty is the valve lift since the pressure against the valve are much greater than in normal operation the lift profile will be altered and the opening of the valve will most likely deviate more than in standard operation. It has been obeserved at Scania in engine test cells that the valve lift is altered when there is significant pressure ratios between cylinder pressure and manifold pressures. In Figures 5.9 and 5.12 it is seen that the peak pressure is too big and that the pressure following past ± 300 CAD is too low. The largest source of error is most likely that the C_D values for exhaust are not measured for the significant pressure ratios between cylinder pressure and exhaust manifold pressure. In Figures 5.10 and 5.13 it is seen that the largest massflow is close to TDC. That is where the pressure ratios between cylinder pressure and exhaust manifold are the greatest and that is were the uncertainty of C_D value and valve lift is most significant. In the pV-diagram, Figures 5.9 and 5.12, it is seen that the simulated pressure captures the physics somewhat but not the pressure peaks. The dashed blue line

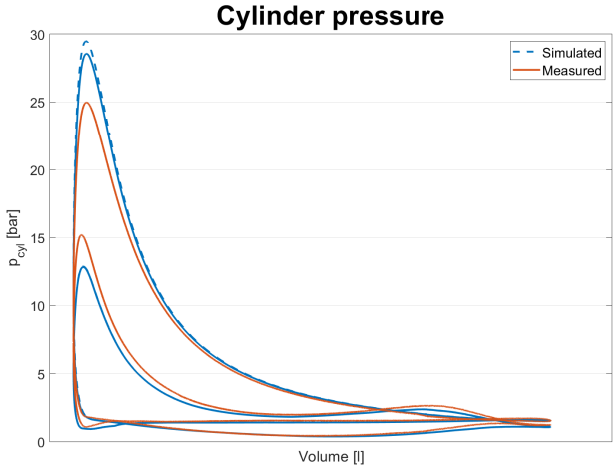

Figure 5.9: *pV diagram CRB 1000 RPM.*

from the simulated which is higher then the solid is from bad inital conditions for temperature and pressure in the cylinder. The solid blue line is what the pV-diagram converges to after some simulations. The VVB measurement at 1000 RPM had average indicated torque of -761 Nm and the simulated not including friction was -736 Nm. At 1700 RPM the measured indicated torque was -1700 Nm and the simulated was -1716 Nm.

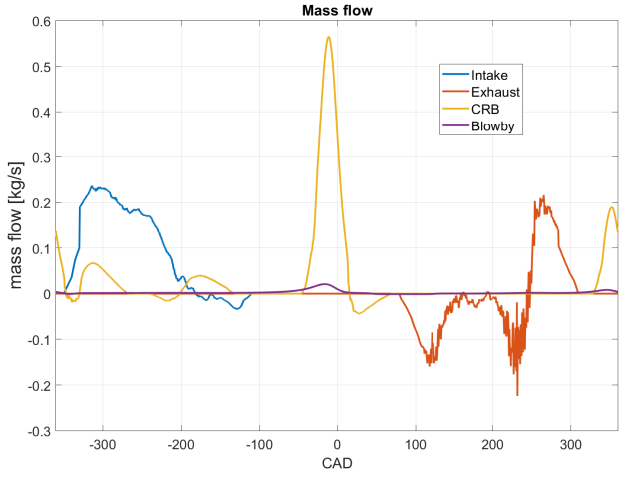

Figure 5.10: *Simulated massflow CRB 1000 RPM.*

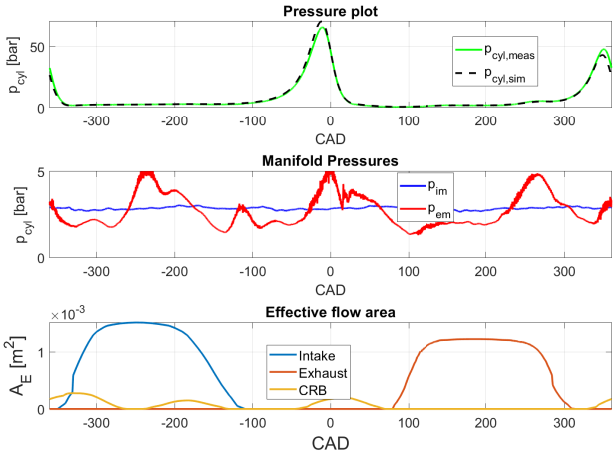

Figure 5.11: *Pressure CAD plot CRB 1700 RPM. The manifold pressures for intake and exhaust are seen. The intake manifold pressure is rather constant while the exhaust manifold pressure have pulses. The effective flow area shows that the CRB is activated.*

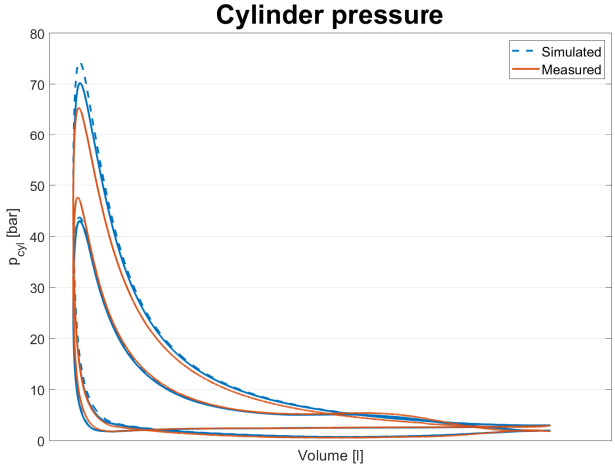

Figure 5.12: *pV diagram CRB 1700 RPM.*

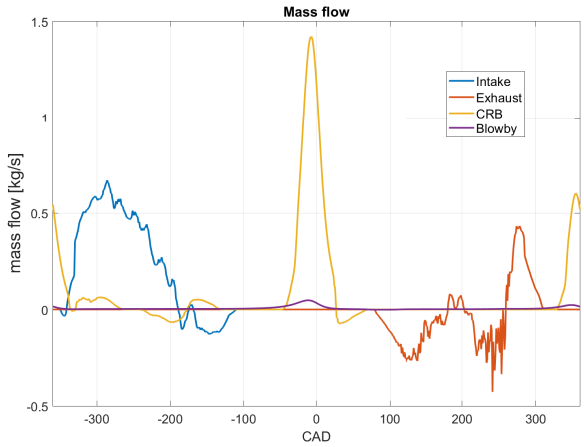

Figure 5.13: *Simulated massflow CRB 1700 RPM.*

5.3 Combustion

In this subchapter the results obtained from combustion simulations are discussed. The data have been collected in an engine cell at high load (~250 mg/stroke fuel), the difference between the two measurements is when the injector needle starts to inject fuel. Meaning that start of injection (SOI) have been altered between the two different measurements. λ measured and simulated is also discussed in this subchapter. λ gives a hint on the trapped mass in the cylinder. That is if the mass of fuel m_f and $(A/F)_s$ is known see the definition of λ in equation (2.33). Thereby λ can give a hint how well the gas exchange works within the model.

Another measurement is at low load (~38 mg/stroke fuel). In all combustion measurements discussed here the engine speed was 1200 RPM. In Figure 5.14 the simulation captures the physics but one can clearly see that the simulated pressure curve starts to burn too late. The measured λ in that case was 1.853 while the simulated was 1.879. The reason for the difference might be that simulated and engine test cell might not use the same value of $(A/F)_s$ or that the estimated mass at IVC in the simulation might be a little off. In the pV-diagram Figure 5.15 it is seen that both the gas exchange as well as the peak pressure is captured, however the expansion polytrope is somewhat off compared to the measured. Compared to previous massflows the massflow in Figure 5.16 is much greater. That is mostly due to that fact that the p_{im} pressure is greater as consequence of the increase in boost pressure from the turbocharger. The measured indicated torque was 2499 Nm and the simulated was 2560 Nm from Figure 5.15. Figure 5.17 shows the massfraction of air, when the combustion starts the massfraction of air decreases. At IVO the cylinder is filled with fresh

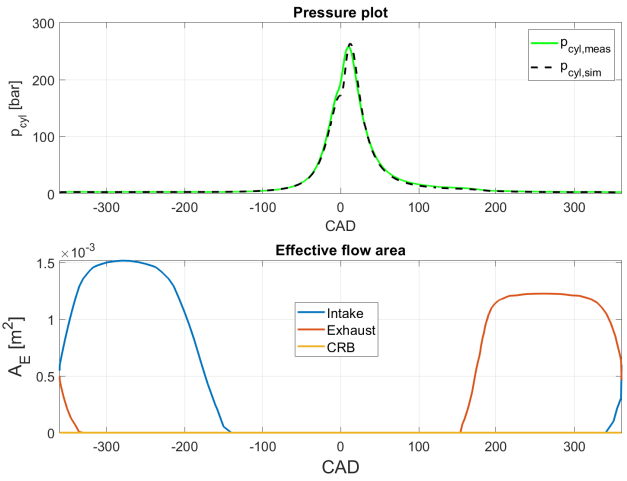

Figure 5.14: *CAD pressure plot for high load 2500 Nm.*

air wich increases the mass fraction of air as seen in the Figure.

The simulated pressure curve in Figure 5.18 shows the cad pressure curve and effective flow area at high load at 1200 RPM. The simulated pressure curve captures the shape of the measured pressure somewhat. The pressure increase due to combustion is too large in the simulated case. That is most likely due to that Diesel combustion needs at least a double Vibe to be modeled accurately. That is due to the fact that there is a premix and a main burning which cannot be accurately described by a single Vibe. Even though that the pV diagram in Figure 5.19 deviates somewhat from the measured, the average indicated torques measured and simulated are quite close, 2501 Nm and 2572 Nm respectively. The measured λ was 1.898 and the simulated was 1.917, thereby the simulated and measured is close. The torque deviates due to that the torque is measured at the flywheel and thereby friction losses is most likely obtained.

In Figure 5.21 it is seen that the simulated pressure follows both the expansion and compression curve well, but the simulated pressure does not capture the pressure peak. The reason is most likely due to the fact that Matekunas pressure ratio method fails to make an accurate heat release in this case. The pressure difference from compression and combustion in this case is not much at all and thereby a small error in the polytrope in Matekunas will fail to predict an accurate heat release. In the two previous combustion data sets the injected fuel was ~250 mg/stroke compared to ~38 mg/stroke here. In Figure 5.22 it is seen that the gas exchange is well captured by the simulation even though it fails to predict the peak pressure. The gas exchange happens when there is an effective flow area. In those regions in Figure 5.21 the simulated and measured pressure are essentially the same. The simulated massflow in Figure 5.23 shows

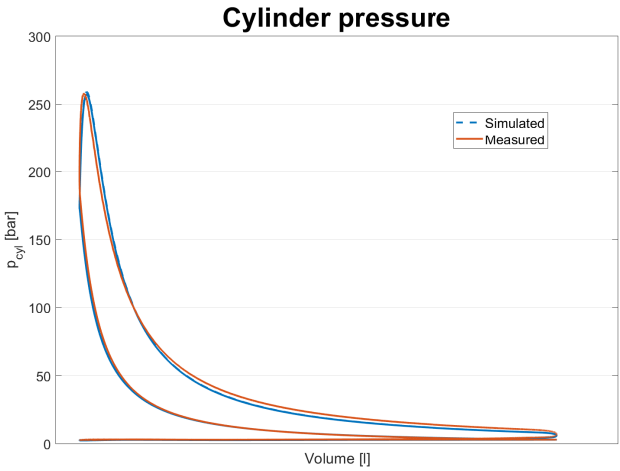

Figure 5.15: *pV diagram for high load 2500 Nm.*

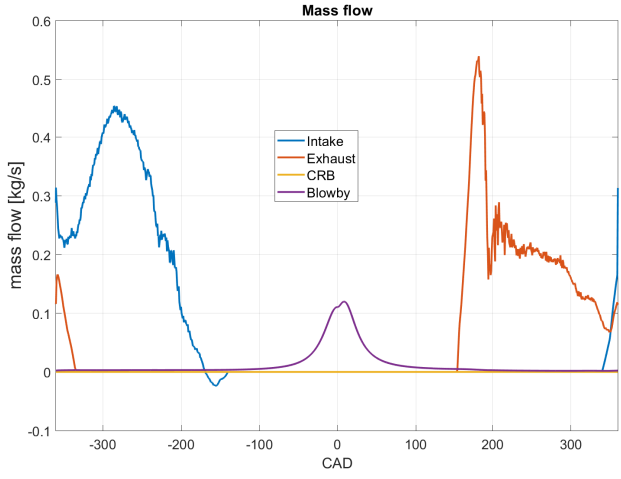

Figure 5.16: *Simulated massflow for high load 2500 Nm.*

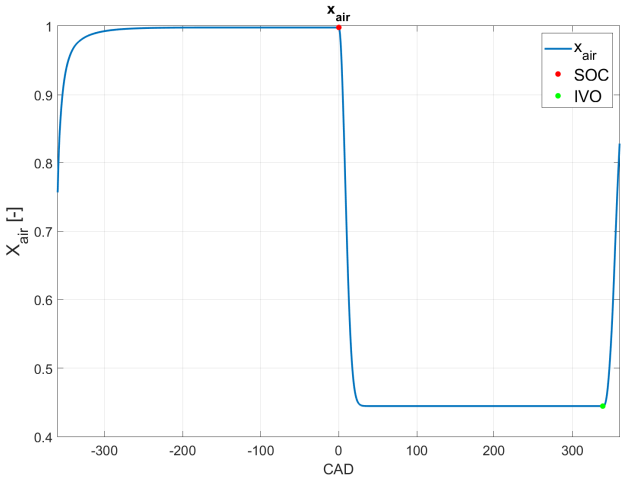

Figure 5.17: *Mass fraction of air at high load 2500 Nm.*

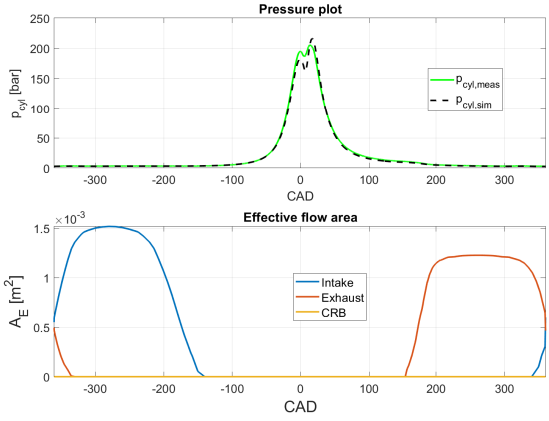

Figure 5.18: *CAD pressure plot for high load 2500 Nm.*

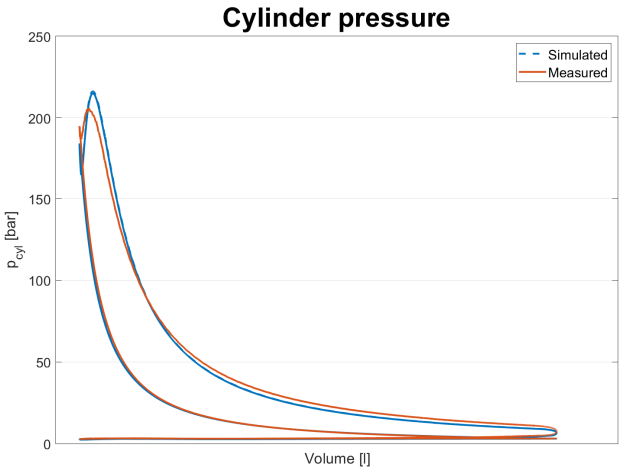

Figure 5.19: *pV diagram for high load 2500 Nm.*

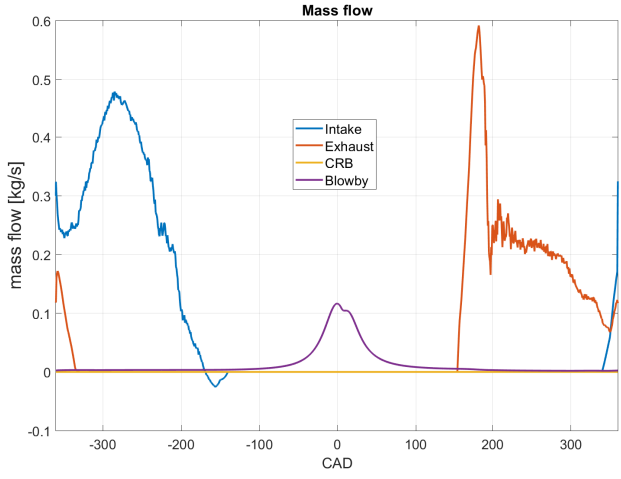

Figure 5.20: *Simulated massflow for high load 2500 Nm.*

oscillations in the mass flow from the intake valve which suggest that the pressure in the intake manifold and the cylinder are close to each other causing numeric instabilities as described in Chapter 2.6.1. The measured indicated torque from Figure 5.22 was 171 Nm and the simulated was 182.2 Nm.

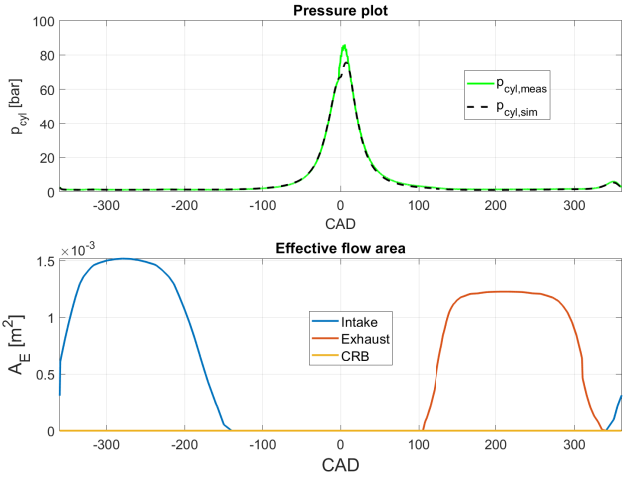

Figure 5.21: *CAD pressure plot for low load 170 Nm.*

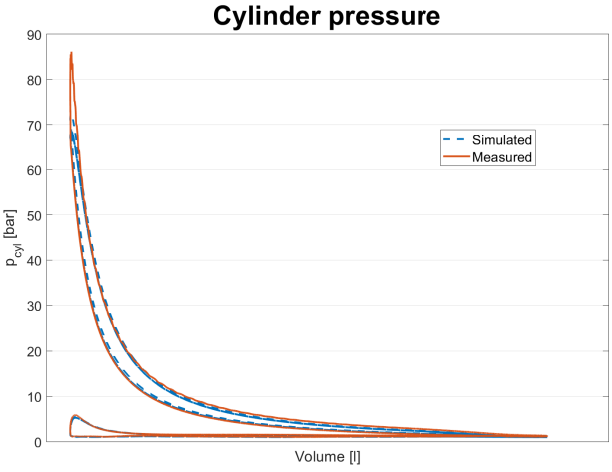

Figure 5.22: *pV diagram for low load 170 Nm.*

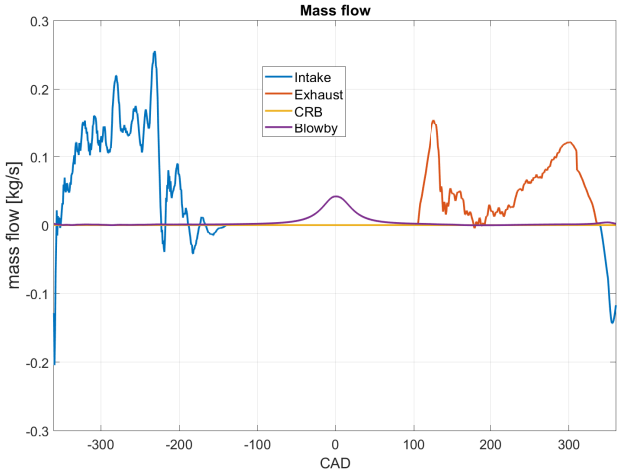

Figure 5.23: *Simulated massflow for low load 170 Nm.*

In Figure 5.24 it is seen that the mass fraction of air does not increase at IVO. That has to do with the fact that there is backflow to the intake manifold. Hence there is no flow of fresh air into the cylinder, and with the assumption that the mixture is homogeneous the mass fraction of air is unaltered.

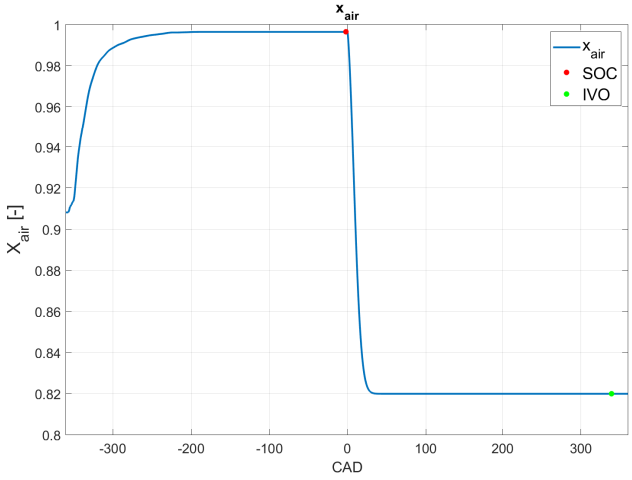

Figure 5.24: *Mass fraction air for low load 170 Nm.*

5.4 Real Time Feasibility Study

The purpose of this study was to see if it is possible to implement the model on a HIL environment for functional testing and if it is possible to implement on an ECU. The test was performed on a data set with combustion. The runtime was estimated by using `Tic` and `Toc` in Matlab. To be able to get as realistic result as possible the Simulink model was built before the run time estimation was perfomed. That was solved in Simulink by the use of `enable fast restart`. The runtime for different solvers and step lengths are presented in Table 5.1. The test used here only used fixed step length and that is essential for implementation on ECU but not required on HIL. The simulation time obtained and the step lengths used, suggest that it is possible to implement the model on a HIL environment and on an ECU by code optimization.

Table 5.1: *Runtime for different solvers on the simulink model on a portable computer with Intel I5 2.5 GHz 8GB RAM, the simulation time was set to 1 second. By fail it is meant that the simulation crashes.*

Step length h	**ODE1 [s]**	**ODE2 [s]**	**ODE4 [s]**
$4 \cdot 10^{-4}$	fail	fail	fail
$3 \cdot 10^{-4}$	fail	0.98	1.01
$2 \cdot 10^{-4}$	1.03	1.08	1.14
$1 \cdot 10^{-4}$	1.31	1.43	1.99
$5 \cdot 10^{-5}$	1.78	2.15	3.24
$1 \cdot 10^{-5}$	6.27	7.36	10

6
Future Work

The valve lifts discussed in this thesis have been measured for a cold engine and by turning the camshaft two revolutions. However as the engine gets warmer the valves get longer and thereby does not agree with the measured valve lifts. Fortunantely there are methods to compensate for that, for instance by hydraulic lash adjusters (HLA). The HLA reduces the maintenance significantly, as the need for periodically adjusting the valve lash disappear (Phlips and Schamel, 1991). The valve lift affects the mass flow through the ports and thereby it is essential to know the true valve lift. By using HLA, EVO and IVO can be more accurately determined.

The C_D values needs to be measured for larger pressure ratios for the exhaust valve. There is also a need to make transient measurements. It has been concluded in Winroth et al. (2018) that the C_D values measured from stationary measurements are overestimated. By transient experiment it is meant that the air flow rig uses the same valve motion and under the same conditions as an engine would have done. The stationary measurements are that the valve is lifted into position and the massflow is observed when it has reached a static level.

The Simulink model uses the temperature in the exhuast manifold as input and uses it for the flow calculation at the exhaust port. The engine studied in this thesis had temperature sensors at the exhaust ports however the engines in production does not. Thereby a model for the temperature in the exhaust manifold would be necessary. It would be interesting to perfom a sensitivity analysis and see how important it is to get the temperature correct or if it is good enough to set the temperature to a constant.

A further investigation of this thesis would also be to implement the model in an ECU and see if it is possible to do so from the step lengths needed for the model.

In this thesis a goal was that the model should use the same set of equations for all different parts of the four stroke cycle. From an ECUs point of view it is good, because the simulation time will not vary as much as if there were different calculations for the different cases. The model as of now does its calculations in the time domain. A simple scaling of $\frac{1}{\omega_e}$ is what is needed to change the model to calculate in the crank angle domain. A limitation if the model would calculate in the crank angle domain would be how to handle the case when the engine speed $\omega_e = 0$. That is not a problem for the Simulink model since it is in the time domain.

A state for piston temperature and wall temperature is needed to get a better heat transfer model. The piston temperature will affect the ring gap which in turn will affect the blowby flow. An investigation on how the ring gap affect the blowby flow would be interesting. The wall temperature could by knowing material and the temperature in the cylinder act as a state as for piston temperature. Guzzella and Onder (2010) suggests that the wall temperature T_w can be estimated by looking at the increase in temperature in the coolant and from knowing the coolants flow rate.

In Chapter 2.9 it is described that diesel combustion in DI engines requires at least a double Vibe to accurately model the combustion. To be able to parameterise those two Vibe functions a more accurate heat release analysis has to be performed, for example by studying the gross heat release which compared to the net heat release also considers contribution from heat transfer. A more accurate way to determine the SOC is also required either by using the models for ignition delay from chapter 2.8.1 or by analysing cylinder pressure data.

Another interesting investigation would be to run the simulation model on the other cylinders that are not closest to the flywheel. Thereby it could be seen how sensitive the model is for the torsion and flexibility in the crankshaft.

Finally a modification that the instantaneous volume V is not only dependent on θ but also p_{cyl}. That because the instantaneous cylinder volume can deviate as much as 6% from the geometrical at TDC at high load (Anagrius West et al., 2018). At high load the forces acting on the piston makes the piston deviate somewhat from its provided geometrical data.

Appendix

A

Model Parameters

This appendix presents some of the different model parameters that have been used in this thesis.

A.1 Gas Properties

Table A.1 show the mole mass for some common species. Atmospheric nitrogen is that the gases that makes up air except for oxygen have been lumped into nitrogen. The air model in equation (2.20) gives the following molar mass for air:

$$M_{air} = \frac{1}{1 + 3.773}(1 \cdot 32 + 3.773 \cdot 28.16) = 28.96 \text{ [g/mole]} \tag{A.1}$$

The mole mass for the burned gases is (assuming that cetane is the fuel a=16, b=34):

$$\begin{aligned} M_{\text{Burned}} &= \frac{1}{a + \frac{b}{2} + 3.773(a + \frac{b}{4})}(aM_{CO_2} + \frac{b}{2}M_{H_2O} + 3.773(a + \frac{b}{4})M_{N_2}) = \\ &= \frac{1}{16 + 17 + 3.773 \cdot (16 + 34/4)}(16 \cdot 44.01 + 17 \cdot 18.02 + 3.773 \cdot (16 + 34/4) \cdot 28.16) = \\ &= 28.81 \text{ [g/mole]} \end{aligned} \tag{A.2}$$

Since the mole mass of air and burned gases do not differ much the mass specific gas constant R is roughly the same for air as for burned gases.

Table A.1: *Molar mass from species taken from Heywood (2019).*

Specie	Molecular weight [g/mole]
Carbon C	12.011
Hydrogen H_2	2.016
Cetane $C_{16}H_{34}$	226.44
Oxygen O_2	32.00
Atmospheric Nitrogen N_2	28.16
Carbon dioxide CO_2	44.01
Water H_2O	18.02

A.2 Valve Properties

The valve lift profiles L_v shown in Figure A.1 is used when calculating the C_D values for exhaust, intake and CRB. The lift profile for CRB and exhaust at high pressure ratios will differ from the values obtained from the look up table, however that has not been considered in the implementation. The C_D values displayed in Figures A.2 and A.3 have been measured at steady flow experiments.

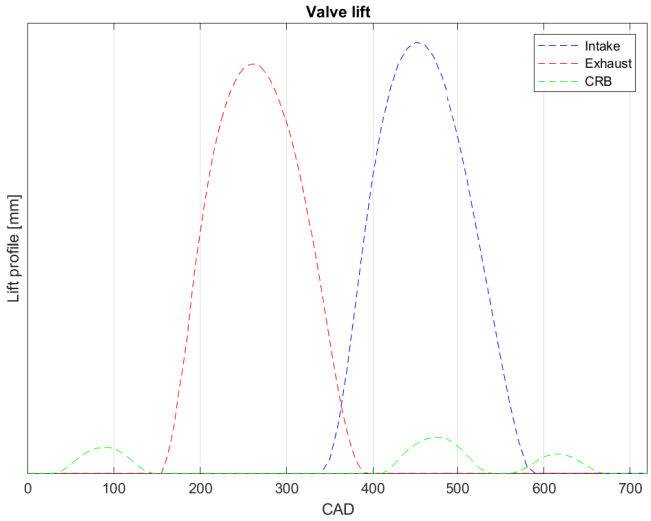

Figure A.1: *Valve lift for the different valves note that TDC fire is at 360 °.*

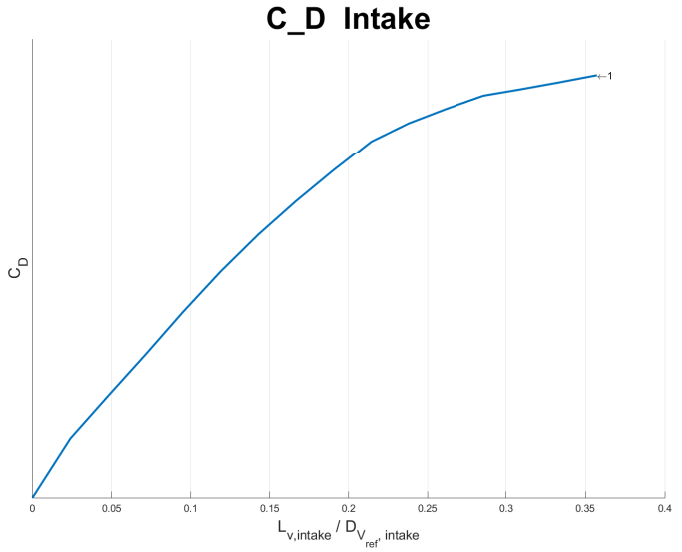

Figure A.2: *C_D value for intake valve as a function of L_v/D_v*

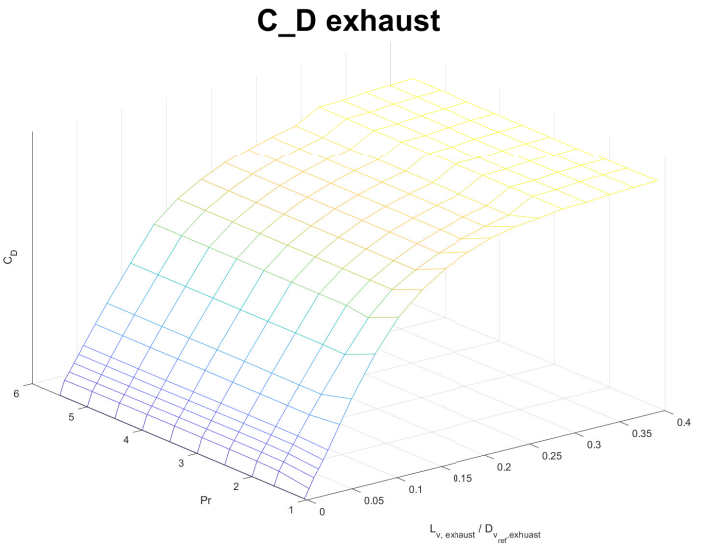

Figure A.3: *C_D value for exhaust valve as a function of L_v/D_v and Pr (pressure ratio).*

Bibliography

Ivan Anagrius West, Carlos Jorques Moreno, Ola Stenlåås, Fredrik Haslestad, and Ola Jönsson. Internal combustion engine cylinder volume trace deviation, apr 2018. Cited on pages 8 and 56.

Yunus A. Cengel, Mehmet Kanoglu, John M. Cimbala, and Robert H. Turner. *Fundamentals of thermal-fluid sciences.* McGraw-Hill Education, 5 th edition, 2017. Cited on pages 8, 11, and 18.

C Lyle Cummins. *Jacobs Engine Brake Retarder, Bloomfield, Conneticut*. American Society of Mechanical Engineers, 1985. Cited on page 17.

Thomas Dresner and Philip Barkan. A review of variable valve timing benefits and modes of operation. In *1989 Conference and Exposition on Future Transportation Technology*. SAE International, aug 1989. Cited on page 17.

Rolf Egnell. The influence of egr on heat release rate and no formation in a di diesel engine. In *CEC/SAE Spring Fuels & Lubricants Meeting & Exposition*. SAE International, jun 2000. Cited on page 2.

Asko Ellman and Robert Piché. A two regime orifice flow formula for numerical simulation. *Journal of Dynamic Systems Measurement and Control*, 121:721–724, 12 1999. Cited on page 16.

Lars Eriksson. CHEPP – A Chemical Equilibrium Program Package for Matlab. *SAE Transactions, Journal of Fuels and Lubricants, 2004-01-1460*, 4(113):730–741, June 2005. Cited on page 14.

Lars Eriksson and Ingemar Andersson. An analytic model for cylinder pressure in a four stroke si engine. *SAE Transactions*, 111:726, 2002. Cited on pages 2 and 23.

Lars Eriksson and Lars Nielsen. *Modeling and control of engines and drivelines.* Automotive series. Chichester, West Sussex, U.K. : John Wiley and Sons Ltd, 2014. Cited on pages 6, 7, 11, 14, 15, 16, 18, 19, 20, 21, 23, 29, 31, and 32.

J. A. Gatowski, E. N. Balles, K. M. Chun, F. E. Nelson, J. A. Ekchian, and John B. Heywood. Heat release analysis of engine pressure data. In *1984 SAE International Fall Fuels and Lubricants Meeting and Exhibition*. SAE International, oct 1984. Cited on pages 2 and 14.

L. Guzzella and Christopher H. Onder. *Introduction to modeling and control of internal combustion engine systems.* Springer, 2010. Cited on pages 31 and 56.

H.O. Hardenberg and F. W. Hase. An empirical formula for computing the pressure rise delay of a fuel from its cetane number and from the relevant parameters of direct-injection diesel engines. In *1979 Automotive Engineering Congress and Exposition*. SAE International, feb 1979. Cited on page 18.

John Heywood. *Internal Combustion Engine Fundamentals 2E.* New York, N.Y. : McGraw-Hill Education., 2019. Cited on pages 8, 10, 15, 17, 18, 19, 28, 37, and 60.

Bonnie J. McBride, Michael J. Zehe, and Sanford Gordon. Nasa glenn coefficients for calculating thermodynamic properties of individual species. 10 2002. Cited on page 13.

Bengt Johansson. *Förbränningsmotorer del 2.* Lund : Institutionen för värme- och kraftteknik, Lunds tekniska högskola, 2003, 2003. Cited on page 37.

Bengt Johansson. *Combustion engines volume I.* Lund : Lund University ; Stockholm : Kungliga Tekniska Högskolan, KTH, 2017. Cited on page 10.

Felicia Åkerman. Eu:s ledare och parlamentet överens om krav på minskade utsläpp från lastbilar. *Dagens industri*, feb 19 2019. https://www.di.se/live/eus-ledare-och-parlamentet-overens-om-krav-pa-minskade-utslapp-fran-lastbilar/ accessed: 2019-02-20. Cited on page 1.

Marcus Klein and Lars Eriksson. A specific heat ratio model for single-zone heat release models. In *SAE 2004 World Congress & Exhibition*. SAE International, mar 2004. Cited on page 14.

Markus Klein. *Single-zone cylinder pressure modeling and estimation for heat release analysis of SI engines.* Linköping studies in science and technology: Dissertations 1124. Linköping : Department of Electrical Engineering, Linköping University, 2007, 2007. Cited on pages 2 and 22.

R.B. Krieger and G.L. Borman. *The Computation of Apparent Heat Release for Internal Combustion Engines*. American Society of Mechanical Engineers. ASME, 1966. Cited on pages 2 and 20.

Patrick Phlips and Andreas Schamel. The dynamics of valvetrains with hydraulic lash adjusters and the interaction with the gas exchange process. In *International Congress & Exposition*. SAE International, feb 1991. Cited on page 55.

Andrew L. Randolph. Methods of processing cylinder-pressure transducer signals to maximize data accuracy. In *International Congress & Exposition*. SAE International, feb 1990. Cited on page 37.

Gerald Rassweiler and Lloyd Withrow. Motion pictures of engine flames correlated with pressure cards. In *Annual Meeting of the Society*. SAE International, jan 1938. Cited on pages 2 and 21.

Mark C. Sellnau, Frederic A. Matekunas, Paul A. Battiston, Chen-Fang Chang, and David R. Lancaster. Cylinder-pressure-based engine control using pressure-ratio-management and low-cost non-intrusive cylinder pressure sensors. In *SAE 2000 World Congress*. SAE International, mar 2000. Cited on page 2.

Peter Templin. A diesel engine model, including compression brake for, powertrain control. In *International Truck and Bus Meeting and Exhibition*. SAE International, nov 2002. Cited on page 2.

Ivan I Vibe and Franz Meißner. *Brennverlauf und kreisprozess von verbrennungsmotoren*. Verlag Technik, 1970. German translation of the russian original. Cited on page 2.

Johan Wahlström and Lars Eriksson. Modelling diesel engines with a variable-geometry turbocharger and exhaust gas recirculation by optimization of model parameters for capturing non-linear system dynamics. *Proceedings of the Institution of Mechanical Engineers, Part D, Journal of Automobile Engineering*, 225(7):960–986, 2011. Cited on page 30.

Marcus Winroth, C L. Ford, and Per-Henrik Alfredsson. On discharge from poppet valves: effects of pressure and system dynamics. *Experiments in Fluids*, 59, feb 2018. Cited on page 55.

G. Woschni. A universally applicable equation for the instantaneous heat transfer coefficient in the internal combustion engine. In *National Fuels and Lubricants, Powerplants, Transportation Meetings*. SAE International, feb 1967. Cited on pages 2 and 31.